

Dual Function of NRP1 in Axon Guidance and Subcellular Target Recognition in Cerebellum

Highlights

- SEMA3A attracts basket cell axons expressing NRP1 in vitro and in vivo
- NRP1 interaction in *trans*, but not in *cis*, with NF186 directs AIS innervation
- NRP1 mediates both axon guidance and adhesion during GABAergic synapse formation
- NRP1 interaction with SEMA3A and NF186 occurs on distinct domains

Authors

Ludovic Telley, Christelle Cadilhac, Jean-Michel Cioni, ..., Alexandre Dayer, Andrea B. Huber, Fabrice Ango

Correspondence

fabrice.ango@igf.cnrs.fr

In Brief

The molecular mechanisms underlying GABAergic subcellular synapse targeting are not fully understood. Telley et al. reveal that the SEMA3A receptor neuropilin-1 directs both axon guidance and target recognition through timely molecular interaction during local GABAergic circuit formation.



Dual Function of NRP1 in Axon Guidance and Subcellular Target Recognition in Cerebellum

Ludovic Telley,^{1,2,3,4,9} Christelle Cadilhac,^{1,2,3,4,9} Jean-Michel Cioni,^{1,2,3,5} Veronique Saywell,^{1,2,3} Céline Jahannault-Talignani,^{1,2,3} Rosa E. Huettl,⁶ Catherine Sarrailh-Faivre,⁷ Alexandre Dayer,^{4,8} Andrea B. Huber,⁶ and Fabrice Ango^{1,2,3,10,*}

¹Department of Neurobiology, Institut de Génomique Fonctionnelle, CNRS, UMR5203, 34090 Montpellier, France

²INSERM, U1191, 34094 Montpellier, France

³Université de Montpellier, 34090 Montpellier, France

⁴Department of Basic Neurosciences, University of Geneva Medical School, CH-1211 Geneva 4, Switzerland

⁵Department of Physiology Development and Neuroscience, University of Cambridge, Anatomy Building, Downing Street, Cambridge CB2 3DY, UK

⁶Institute of Developmental Genetics, Helmholtz Zentrum München–German Research Center for Environmental Health, 85764 Neuherberg, Germany

⁷Aix-Marseille Université, CNRS, CRN2M-UMR7286, 13284 Marseille, France

⁸Department of Mental Health and Psychiatry, University of Geneva Medical School, CH-1211 Geneva 4, Switzerland

⁹Co-first author

¹⁰Lead Contact

*Correspondence: fabrice.ango@igf.cnrs.fr

<http://dx.doi.org/10.1016/j.neuron.2016.08.015>

SUMMARY

Subcellular target recognition in the CNS is the culmination of a multiple-step program including axon guidance, target recognition, and synaptogenesis. In cerebellum, basket cells (BCs) innervate the soma and axon initial segment (AIS) of Purkinje cells (PCs) to form the pinceau synapse, but the underlying mechanisms remain incompletely understood. Here, we demonstrate that neuropilin-1 (NRP1), a Semaphorin receptor expressed in BCs, controls both axonal guidance and subcellular target recognition. We show that loss of Semaphorin 3A function or specific deletion of NRP1 in BCs alters the stereotyped organization of BC axon and impairs pinceau synapse formation. Further, we identified NRP1 as a trans-synaptic binding partner of the cell adhesion molecule neurofascin-186 (NF186) expressed in the PC AIS during pinceau synapse formation. These findings identify a dual function of NRP1 in both axon guidance and subcellular target recognition in the construction of GABAergic circuitry.

INTRODUCTION

Adequate functioning of neuronal circuits relies on the formation of specific synaptic connections among different classes of neurons. This is illustrated well by the ability of local inhibitory interneurons to modulate information that is dispatched by long-range principal neurons within brain networks. The repertoire of inhibitory coding strategies is greatly expanded by the diversity of GABAergic interneurons that display specific synaptic

connectivities onto distinct cellular and subcellular targets. A striking example of developmental synaptic specificity is provided by two classes of GABAergic interneurons: the basket (BC) and chandelier cells, which contact principal cells at their soma and axon initial segment (AIS), respectively (reviewed in Freund and Buzsáki, 1996; Huang et al., 2007). To date, the cellular and molecular mechanisms underlying such subcellular innervation specificity remain largely unknown.

Wiring specificity is the culmination of sequential developmental processes that include cell migration, axon guidance, target recognition, and synapse formation. For GABAergic interneurons, some research groups have proposed that these neurons seek their target with high precision based on extracellular guidance cues (Betley et al., 2009; Stepanyants et al., 2004), while other groups have stated that coordinated growth of pre- and postsynaptic structural elements, occurring independently from extracellular cues, is sufficient to control local innervation patterns (Li et al., 2007). In the latter case, the proximity of GABAergic interneurons with their cellular targets is sufficient to allow specific inhibitory connectivity.

In cerebellar cortex, Purkinje cells (PCs) receive two sets of GABAergic inputs, one from BCs and the other from stellate cells (SCs) (Sotelo, 2008). SCs selectively innervate PC dendritic shaft and spines, while BCs project abundantly to PC AIS, forming the so-called pinceau synapses (Ramon y Cajal, 1911). Pinceau synapse is formed by locally exuberant terminal branching that is controlled by the axon guidance molecule Semaphorin 3A (SEMA3A) through activation of a specific src kinase FYN signaling pathway (Cioni et al., 2013). The specificity of this subcellular innervation pattern could be explained by the proximity of BCs to PC soma and AIS, and SCs to PC dendrites in the mature cerebellar cortex (Sotelo, 2008). To further examine this hypothesis, we investigated whether axons of BCs are instructed by extracellular cues to reach the PC layer (PCL) and how subcellular target recognition is specified locally. We found that

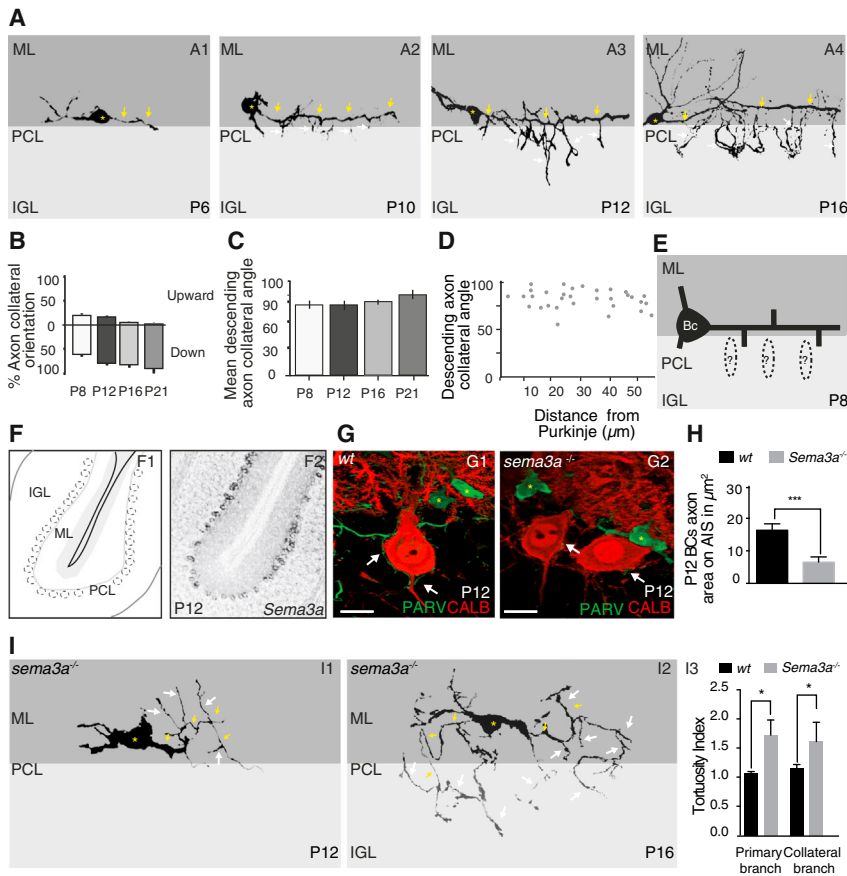


Figure 1. Aberrant Axon Organization in *sema3a*^{-/-} Deficient Mice

(A) BC axon development during pinceau synapse formation. Camera lucida-like reconstruction of typical BC axon organization visualized with GFP in B20 BAC transgenic mice at P6 (A1), P10 (A2), P12 (A3), and P16 (A4). Note that from BC axon shaft (yellow arrows), several BC axon collaterals emerged with a rather straight path to PCs (white arrows).

(B–D) Quantification of axon collateral orientation (B) showed that 50%–80% displayed a descending orientation toward PCL at all observed developmental stages (P8–P21). These collaterals emerged at a mean of $(89.7^{\circ} \pm 6.4^{\circ})$ (from BC axon shaft, as quantified in C). The same collateral angle and orientation are observed for BCs independently of their position in the ML and the distance from PC somata (D).

(E) Schematic representation of characteristic BC axon organization and targeting toward PC soma. (F) Schematic representation of one folium of cerebellum (F1). *Sema3a* in situ hybridization at P12 showed strong expression in PC somata (F2). (G and I) BC axon organization was visualized with PARV (G) or Golgi staining (I) in both WT (G1) and *sema3a*^{-/-} (G2 and I) at P12 (G and I1) or P16 (I2). White arrows showed BC axon collaterals at both soma and AIS. Yellow arrows showed BC axon main shaft (I). Note that collateral position and tortuosity are totally aberrant in *sema3a*^{-/-} (I1–I3; **n* = 10, *p* = 0.005, Student's *t* test).

(H) Quantification of pinceau area at AIS in both WT and *sema3a*^{-/-} revealed a statistically significant increase in primary and collateral branches at P12 in *sema3a*^{-/-} (***n* = 10, *p* = 0.002, Student's *t* test). ML, molecular layer; PCL, Purkinje cell layer; IGL, internal granule cell layer. Scale bars represent 10 μm.

the stereotyped organization of BC axons was dependent on the Semaphorin axon guidance receptor, neuropilin-1 (NRP1). Using both in vitro and in vivo approaches, we demonstrate that local expression of the molecular cue, SEMA3A, controls BC axon pathfinding. Furthermore, NRP1, the obligate receptor for SEMA3A expressed by BCs, is subsequently involved in specific innervation of PC AIS by directly interacting with the cell adhesion molecule NF186. Together, these data indicate that NRP1 provides a molecular bridge for the transitional step between axon guidance and target recognition during GABAergic circuit assembly in the cerebellum.

RESULTS

Early Bias Orientation of BC Axons during PC AIS Innervation

Stereotyped BC axon layout consists of a horizontal main branch that runs parallel to the PCL and several collaterals that are targeted to PC soma and AIS (Palay and Chan-Palay, 1974). As a first step to understand how this target specificity does emerge, we analyzed early developmental time points using bacterial artificial chromosome (BAC) transgenic mice expressing GFP (*gad67::Gfp*) in a subset of BCs (Ango et al., 2008). At postnatal

day 6 (P6), BCs first grew a main horizontal shaft in the molecular layer (ML) with subsequent emergence of collaterals at later developmental ages (Figure 1A). Quantification of BC collateral orientation revealed that $64.3\% \pm 2.6\%$ at P8, $74\% \pm 1.7\%$ at P12, $76.2\% \pm 1.9\%$ at P16, and $85.7\% \pm 1.8\%$ at P21 of them were already topographically biased for the PCL location and displayed a fairly straight descending axis toward the PC soma across every developmental stage observed from P8 to P21 (*n* = 10 cells for each time point; Figure 1B). During this period, only a few collateral branches grew in the opposite direction toward the ML and underwent very little morphological changes, as compared to branches that formed the pinceau synapse with exuberant local terminal branching (Figure 1A). Another distinctive feature of BC axon collaterals is that they emerged at near right angles (*n* = 15 cells per time point, $89.7^{\circ} \pm 6.4^{\circ}$) from the main axonal shaft (Figures 1A, 1C, and 1D). Thus, our data revealed that the mature BC projection pattern emerges from unambiguous directionality of axon collaterals toward PC soma during early postnatal development, rather than by exuberant growth followed by pruning. These results suggested that BC axon growth was guided by local cues originating from PCs rather than from cell-cell interaction. Indeed, if cell-cell interactions were involved in BC axon organization, axon collateral

orientation should be more precise in BCs close to PCs than in BCs far from PCs. To test this issue, we analyzed the directionality of BC collaterals in the ML. Since no correlation was found between the angle of descending BC axon collaterals and distance of PCs (Figure 1D), we hypothesized that an extracellular cue was involved in innervation of PCs by BCs. This prompted us to investigate the nature of such molecular cues (Figure 1E).

Aberrant BC Axon Organization in *sema3a*-Deficient Mice

We recently performed a survey of all classical axon guidance cues (i.e., Netrin, Slit, Semaphorin, and Ephrin) expressed by PC using qRT-PCR approach during postnatal development (Saywell et al., 2014). We identified the secreted axon guidance molecule SEMA3A as a potential candidate since it was the only secreted guidance cue that displayed an expression profile matching with BC axon development. In situ hybridization performed at P3, P8, P12, and P16 (Figures 1F and S1, available online) and Allen brain data analyses (Lein et al., 2007) confirmed our observation of restricted expression of *Sema3a* mRNA in PCs. In addition, we and others recently showed that secreted SEMA3A protein was enriched around PC soma during cerebellar development (Figures S1B–S1G) (Carulli et al., 2013; Cioni et al., 2013). This further identified SEMA3A as a candidate for BC axon organization.

To assess a role of SEMA3A in GABAergic axon guidance, we analyzed BC axon organization in *sema3a*^{-/-} mice (Taniguchi et al., 1997). In wild-type (WT) mice, BC axons labeled with parvalbumin (PARV) enwrapped the soma of PCs and sent their terminal endings to the PC hillock (Figure 1G1). In *sema3a*^{-/-} mice, BCs failed to send their axons around the cell soma and axon hillock of PCs (Figures 1G2 and 1H; **n = 10 cells, p = 0.002, Student's t test). This was not due to BC mislocalization because labeled BC somata were clearly visible in the immediate vicinity of *sema3a*^{-/-} PCs, as is the case in WT mice (Figure 1G). Similarly, the number of PARV-expressing interneurons was not significantly different in the ML of *sema3a*^{-/-} and WT mice (Figure S1H). Because we previously showed that a SEMA3A-FYN-dependent mechanism was responsible for terminal axon branching (Cioni et al., 2013), we wondered whether the reduced axonal localization of BCs at PC soma and AIS was due to early defect in terminal axonal branching rather than mislocalization or aberrant axon collateral branching. For this purpose, we analyzed a single BC axon in SEMA3A-deficient mice. Using rapid Golgi staining, we observed a severe disorganization of BC axon shaft and collaterals (Figure 1I). *Sema3a*^{-/-} BC axons lost both their characteristic horizontal shaft organization and straight collateral descending paths toward PCL, and displayed aberrant tortuosity in the ML (Figure 1I; *n = 10, p = 0.005, Student's t test). This phenotype was also revealed in BCs as a population using the pan-axonal antibody SMI-312, which specifically labels phosphorylated neurofilaments in BC axons (Buttermore et al., 2012) (Figures S1I–S1K; **n = 14, p = 0.0045, Student's t test). Thus, SEMA3A is required for BC stereotyped axonal organization.

Ectopic SEMA3A Redirects BC Axons In Vivo

The defect in BC axon organization observed in *sema3a*^{-/-} mice suggests an instructive role of SEMA3A in BC axon pathfinding.

To further characterize such a role of SEMA3A, we developed a mixed culture of GFP-expressing ML GABAergic interneurons and SEMA3A-expressing Chinese hamster ovary (CHO) cells (Figures S2A and 2A) (Biederer and Scheiffele, 2007). With this assay, we assessed how SEMA3A expression shapes BC axons in vitro (Figures 2A and 2B; Experimental Procedures) (Stepanyants et al., 2004). In fields with CHO cells expressing TOMATO, BC axonal terminals were equally distributed in each quadrant (Figures 2A and 2C). However, fields with higher density of SEMA3A-expressing CHO cells received a larger number of axonal endings (Figure 2C; ***n = 18, p = 0.0006, two-way ANOVA). Because SEMA3A induced local basket axon branching through an FYN-dependent signaling pathway (Cioni et al., 2013), we wondered whether the local increase in axonal endings was due to axon branching rather than axon guidance. Thus, we performed the same experiment in the presence of *fyn*-siRNA (small interfering RNA) to inhibit the formation of axonal branches. In this condition, BC axon endings were also preferentially distributed in quadrant-expressing SEMA3A (Figures S2B–S2E; ***n = 20 cells per condition, p = 0.0009, two-way ANOVA), suggesting that BC axon guidance is mediated through SEMA3A independently of FYN signaling. To corroborate this finding, we analyzed BC axon tortuosity in *fyn*^{-/-} mice at single-cell resolution. We found that both BC primary and collateral branches displayed the same tortuosity index as in control mice (Figures S2F–S2H), further suggesting that BC axon pathfinding was independent of FYN signaling.

The effect of SEMA3A was specific to GABAergic axons since it was observed in neurites labeled with the specific BC axonal marker SMI-312 (Figures S3A1, 2D, and 2E), but not in neurites labeled by the microtubule-associated protein 2 (MAP-2) dendritic marker (Figures S3A2, 2D, and 2E). These effects were specific to SEMA3A because of the following reasons. First, they were not observed with the cell adhesion molecules of the L1CAM family, NF186 or NRCAM, which are expressed by PCs and involved in BC axon extension and targeting (Buttermore et al., 2012) (Figure 2C). Second, when SEMA3C, a functionally similar class 3 Semaphorin, was expressed in CHO cells, we observed a repulsion effect on BC axons that was opposite to the attractive effect of SEMA3A on BC axons (Figures S3B and S3C; ***n = 15, p = 0.0009, two-way ANOVA). Together, these findings indicate that SEMA3A instructs BC axon-specific layout in vitro.

To further characterize the role of SEMA3A in BC axon guidance in vivo, we grafted CHO cells expressing SEMA3A into the developing cerebellum (Figure 2F) and reasoned that this naive source of recognition cue should attract the GABAergic axons. A total of 10⁴ CHO cells were injected at P8, a period when BC axon develops, and effects analyzed at post-injection days (PID) 7 and 14 (Figures 2G and 2H). In control conditions, injected CHO cells expressing TOMATO induced no effect on BC axon (Figure 2H). Interestingly, the CHO cells were incorporated at multiple locations in the granule cell layer (GCL) and continued to express the transgene at least for 14 days post-injection. SEMA3A-expressing CHO cells induced aberrant BC axon targeting that correlated with ectopic CHO cell location in the GCL at PID 7 (Figures 2H2a–2H2c, quantified in Figure 2G; *n = 14, p = 0.047, Fisher's test). Further, ectopic expression of SEMA3A in GCL did not alter the general cellular organization

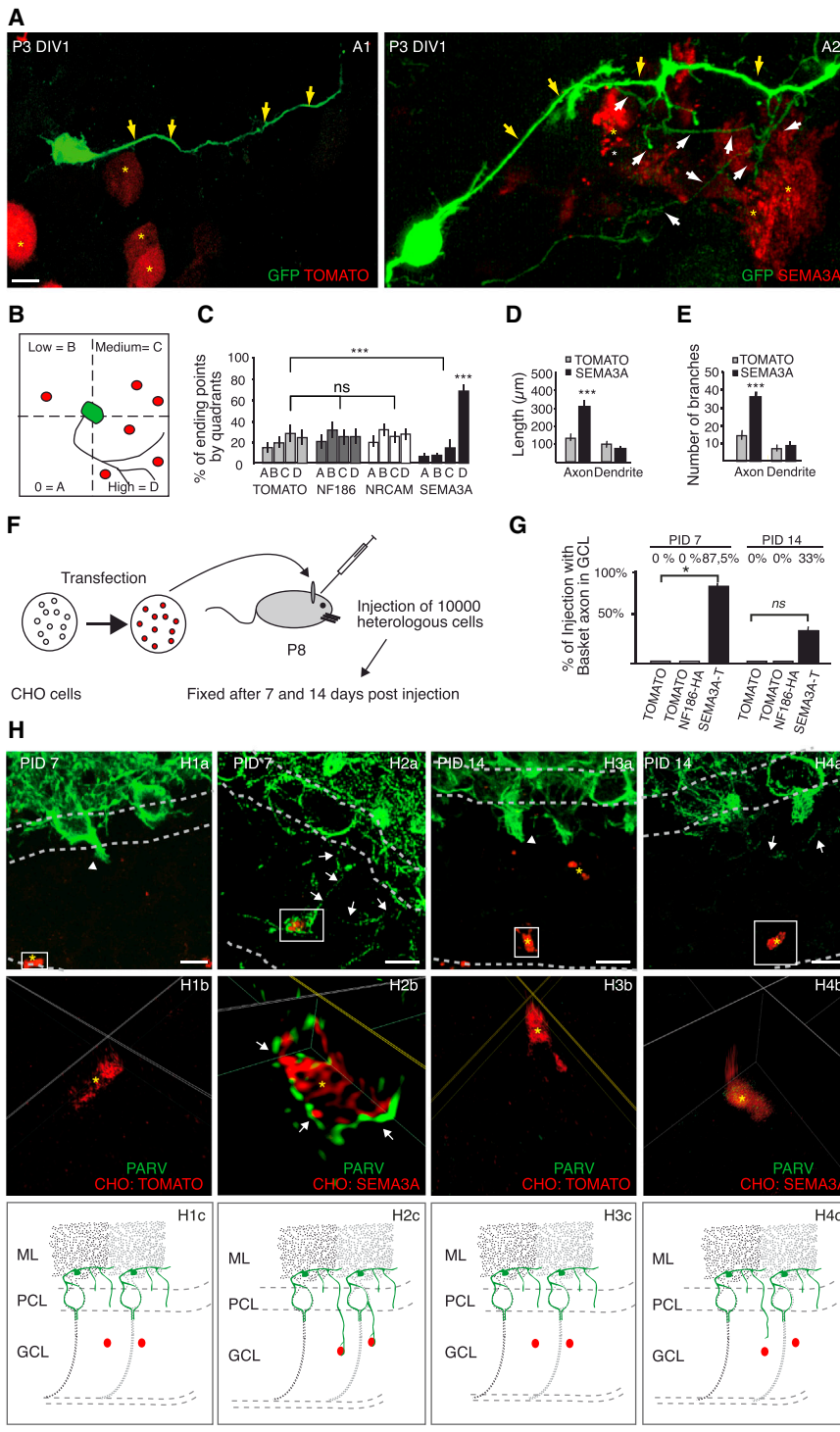


Figure 2. Expression of SEMA3A Is Sufficient to Attract BC Axons In Vitro and In Vivo

(A–C) Co-culture of GFP-labeled cerebellar interneurons mixed with CHO cells transfected with control TOMATO (red; A1) or SEMA3A (red; A2). Schematic representation of the co-culture model with GFP-labeled interneurons (green) and CHO transfected cells in red (B). To quantify axon localization or axon branch preferential localization, images were separated in four equivalent quadrants centered on the neuron soma (B). The number of ending points was counted in each quadrant and scored against the pixel intensity of TOMATO (A1), SEMA3A (A2), or potential attractant candidate for BC axon, NF186, and NRCAM, as quantified in (C). Note that quadrants with high SEMA3A expression level correlate with highest percentage of axonal endings. (C; *** $n = 18$, $p = 0.0006$, two-way ANOVA). Striking BC axon organization with a main shaft and several collaterals that are orientated toward the source of SEMA3A is observed in vitro in the presence of SEMA3A (A2) as compared to control TOMATO (A1). Yellow arrows pointed to BC main shaft, and white arrows showed collaterals. (D and E) Quantification of the length (D) and number of branches (E) in both dendrite and axon.

In the presence of SEMA3A, a 2-fold increase in both length (D; *** $n = 18$, $p = 0.0007$, Student's t test) and axon branches is observed (E; *** $n = 18$, $p = 0.0004$, Student's t test), but not for dendrite. (F) Schematic drawing of the method used to inject CHO cells transfected with molecules of interest in P8 mice.

(G) Quantification of the percentage of BC axons identified in the GCL (PID7 SEMA3A, $n = 14$, $p = 0.047$; PID14 SEMA3A, $n = 9$, $p = 1$, Fisher's test). (H) After 7 (H1 and H2) or 14 (H3 and H4) post-injection days (PID), cerebellar slices are immunostained with PARV antibody (green; H) to reveal interneuron axons. Injection of CHO cells expressing TOMATO (yellow stars in H1 and H3) did not change cerebellar organization and BC axon endings at PC body and AIS (arrowhead; H1a and H3a), as schematized in (H1c) and (H3c). Note that no BC axon can be found in the GCL (H1 and H3) or around CHO cells expressing TOMATO as observed at high magnification in orthogonal views from Imaris software (yellow star; H1b and H3b). Injection of CHO cells expressing SEMA3A triggered ectopic localization of BC axons in GCL 7 PID (H2; white arrows). BC axons can be found deep inside the ML (H2a) and observed around CHO cells expressing SEMA3A-TOMATO at higher magnification in the orthogonal view (arrows; H2b) and as schematized in (H2c). (H4) Note that after 14 PID, BC axons are no longer in the deep GCL, but few axons can be found ectopically near the PCL (white arrows in H4a; schematized in H4c). Scale bars represent 10 μm .

of cerebellar cortex or the morphology of migrating GABAergic interneurons (Figures S4A and S4B). In addition, a time-lapse imaging experiment performed in cerebellar slices injected with SEMA3A-TOMATO or TOMATO revealed that BC migrating behavior and migration speed were similar to that in control slice

(Figures S4C and S4D). Conversely, ectopic expression of SEMA3A in the ML initiated the formation of upward axonal branches that grow toward local SEMA3A (Figure S4E), suggesting that only differentiating interneurons that reached the ML responded to SEMA3A.

The effect of SEMA3A was transient (Figure 2H4). At PID 14, axons retracted from CHO cells, suggesting that other cues were needed to stabilize BC axons (Figures 2H4 and 2G; ns [not significant], $n = 9$, $p = 1$, Fisher's test). No detectable effect was found on BC axon organization in GCL with CHO cells expressing TOMATO alone (Figures 2H1a and 2H1b, schematized in Figure 2H1c). Similar experiments performed with CHO cells expressing NF186 alone showed that NF186 did not instruct GABAergic axons (Figures 2C–2G). Together, these results showed that SEMA3A was sufficient to attract GABAergic axons in vivo.

NRP1 Is Expressed by BCs during Cerebellar Development

SEMA3A signaling requires activation of the holoreceptor, composed of the binding subunit NRP1 and the accessory signaling subunit Plexin A. In view of NRP1 being the cognate receptor of SEMA3A, we sought to determine its expression pattern in postnatal cerebellum. At first, we purified fluorescently labeled BCs (*gad67-gfp* mice, G42 line) at P3, P8, P12, P16, and P21 by using a manual sorting procedure (Saywell et al., 2014) and explored *nrp1* mRNA expression using qRT-PCR (Figure S5A). The presence of *nrp1* mRNA in BCs can be detected from P8 to P21, but not at P3 (Figure S5B). If SEMA3A acts directly on BC axons, NRP1 should be expressed by BCs and localized in the axon. Concomitantly, SEMA3A should be found at BC axon terminals. At P8, we observed strong labeling of SEMA3A at GABAergic interneuron axon endings (Figure S5C). Likewise, in our in vivo grafts of CHO cells expressing SEMA3A-TOMATO, we observed accumulation of SEMA3A-TOMATO protein on BC terminals impinging onto the AIS of PCs (Figure S5D). To further explore NRP1 expression pattern, we used a proximity ligation assay (PLA), a very sensitive technique of amplification that is utilized to detect low levels of protein expression or protein-protein interactions in tissues (see Experimental Procedures). With this approach, we obtained a specific signal for NRP1 in BCs of acute cerebellar slices prepared from WT P8 (Figure S5E), P12 (Figure 3A1), and P21 (Figure 3A3) mice. At P8 and P12, a period when BC axon navigates toward PCs, NRP1 was clearly detected in BC axons, around the PC soma and AIS (Figures 3A1a–3A1c and S7E). At P21, BC axons had fully developed the pinceau and NRP1 expression was maintained precisely in the pinceau area, suggesting an additional role of NRP1 in BC axon organization (Figures 3A3a–3A3c). Together, these results reveal that NRP1 expression in BC axons is consistent with cell-autonomous function of the protein during BC axon layout.

To further confirm implication of NRP1 in BC axon guidance, we bred a conditional NRP1 mutant strain (*nrp1^{fl/fl}*) with a transgenic line expressing the cre recombinase under the control of *ptf1a* promoter (*ptf1a::cre*), which is expressed in BC progenitors during cerebellar development (Hoshino et al., 2005). In the *ptf1a::cre*; *nrp1^{fl/fl}* mouse, NRP1 expression was undetectable in BC axons and was clearly absent in the pinceau (Figures 3A2 and 3A4, as quantified in Figure 3B). Notably, the formation of the mature pinceau was altered (Figure 3A4), highly suggestive of a cell-autonomous function of NRP1 in BC axon layout.

Aberrant BC Axon Organization in *Ptf1a::cre*; *Nrp1^{fl/fl}* Mouse

To further characterize the role of NRP1 in BC axon development, we analyzed the SEMA3A-induced BC axon attraction effect in the presence of selective siRNA against *Nrp1* (Figures 4A2–4C; **** $n = 15$, $p < 0.00001$, two-way ANOVA) or NRP1-blocking antibody (Figure 4C; *** $n = 20$, $p = 0.002$, two-way ANOVA) (He and Tessier-Lavigne, 1997) in the SEMA3A-expressing CHO cell/BC co-culture assay. In both conditions, SEMA3A failed to affect BC axon guidance, showing that SEMA3A-induced BC axon attraction is triggered by NRP1 cell-autonomous expression in BCs.

We performed additional experiments with *ptf1a::cre*; *nrp1^{fl/fl}* mice to evaluate the role of NRP1 in BC axon pathfinding in vivo. We observed a significant reduction of BC axons at the PC AIS (Figures 4D and 4E; * $n = 19$, $p = 0.0183$, Student's t test). To further characterize the role of NRP1 in BC axon organization, we performed Golgi staining in *ptf1a::cre*; *nrp1^{fl/fl}* cerebellar slices at a single-cell resolution. We observed wavy BC principal axon shafts in the ML and poorly developed collaterals in PCL with aberrant tortuosity (Figures 4E2 and 4F; * $n = 10$, $p = 0.0002$, Student's t test). The BC axon phenotype observed in the *ptf1a::cre*; *nrp1^{fl/fl}* was reminiscent of that of *sema3a* knockout mice, thus reinforcing the above hypothesis of a role of SEMA3A in BC axon pathfinding. Since SEMA3A has been recently shown to be involved in climbing fiber synapse elimination during the same developmental stages (Uesaka et al., 2014), we sought to examine if climbing fiber synaptogenesis was also affected in our condition and could thus account for potential indirect effect in BC axon organization. We observed no gross differences in both the morphology and localization of climbing fiber synapses labeled with corticotropin-releasing factor (CRF) and VGLUT2, respectively (Figure S6), suggesting that SEMA3A acted independently on BCs and climbing fibers (Yamano and Tohyama, 1994). Altogether, these data demonstrate that SEMA3A acts directly on NRP1 expressed by BCs during cerebellar development to shape their stereotyped axonal organization.

NRP1 Knockdown in BCs Affects NF186 Localization in PCs

The cell recognition molecule NF186, expressed in Purkinje and basket neurons, regulated cerebellar pinceau organization during postnatal development and was required for proper axon collateral extension and stabilization at AIS (Ango et al., 2004; Buttermore et al., 2012; Zonta et al., 2011). Since pinceau organization was altered in *ptf1a::cre*; *nrp1^{fl/fl}* mice, we wondered whether NF186 (Figure 5A) and ANKG (Figure 5B) expression was also affected. While ANKG (Figures 5A1 and 5A2) expression and localization remained unchanged (Figure 5A3; ns, $n = 14$, $p = 0.77$, Student's t test), NF186 (Figures 5B1 and 5B2) expression pattern at PC AIS was disturbed in *ptf1a::cre*; *nrp1^{fl/fl}* as compared to WT mice. Quantification analyses revealed a significant diffusion of NF186 from AIS and soma toward both proximal dendrite (Figures 5B2 and 5B3; ** $n = 34$, $p = 0.0017$, Student's t test) and axon (Figure 5B3; * $n = 34$, $p = 0.012$, Student's t test) of PCs, as previously observed in ANKG-deficient

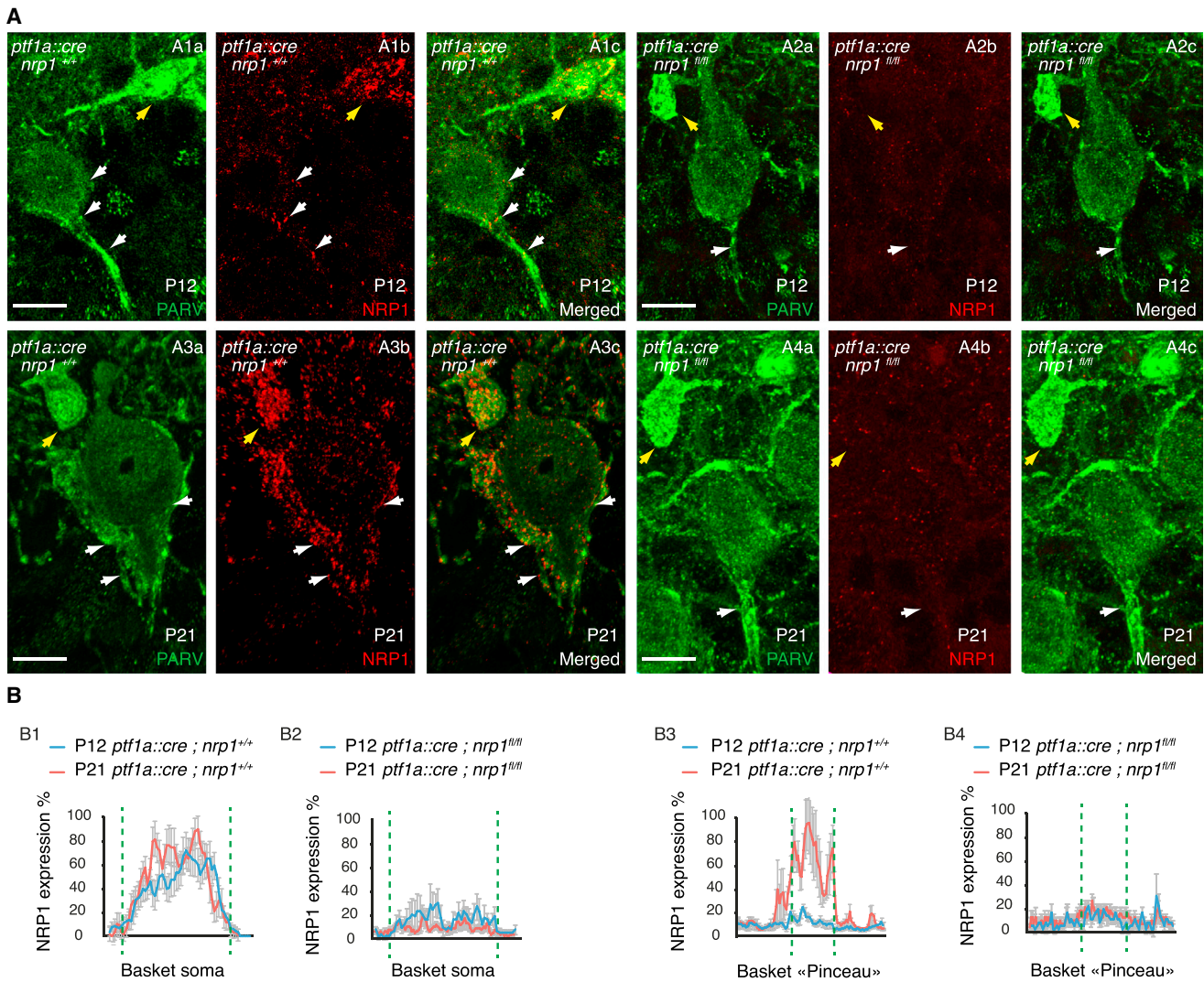


Figure 3. SEMA3A Canonical Receptor Is Expressed by BCs and Preferentially Localized in Pinceau Synapse

(A) PLA immunohistochemistry of NRP1 in both *ptf1a::cre; nrp1^{+/+}* (A1 and A3) and *ptf1a::cre; nrp1^{fl/fl}*, a conditional specific knockout for NRP1 in interneurons (A2 and A4) at P12 (A1 and A2) or P21 (A3 and A4).

(B) Quantification of NRP1 expression. Note that NRP1 localizes in both BC soma (yellow arrowheads) and axon (white arrows at P12; A1 and B1) and is further enriched in pinceau at P21 (A3 and B3). NRP1 expression in BCs is completely lost in *ptf1a::cre; nrp1^{fl/fl}* (A2 and A4), as quantified in (B2) and (B4).

Scale bars represent 10 μ m.

mice (Ango et al., 2004). ANKG is known to limit lateral diffusion of NF186 within the membrane via interaction with the non-phosphorylated form of the tyrosine residue in the FIGQY sequence of NF186 (Garver et al., 1997). We therefore examined the phosphorylation state of NF186 in *ptf1a::cre; nrp1^{fl/fl}* mouse by immunoprecipitation. We observed an increased in tyrosine phosphorylation signals as compared to WT that is supportive of decreased binding with ANKG and increased NF186 lateral diffusion (Figures 5C and 5D; $n = 3$, $p = 0.006$, Student's t test). These results further suggested that NRP1 expressed in BC axon affects NF186 localization in PCs by controlling its level of phosphorylation.

NRP1 and NF186 *trans*-Interact during Pinceau Formation

In addition to modulation of Semaphorin signaling through specific interaction with Plexin A, NRP1 was originally described to mediate cell adhesion (Takagi et al., 1995). We therefore hypothesized that during development, NRP1 involved in BC axon guidance could subsequently control recognition and maintenance of axon contact by interacting with NF186 or NRCAM expressed at PC AIS. To investigate this possibility, NRP1-Fc binding assays were performed in HEK293 cells transiently transfected with NRCAM or NF186 (Figure 6A). We found that NRP1-Fc strongly bound to HEK293 cells

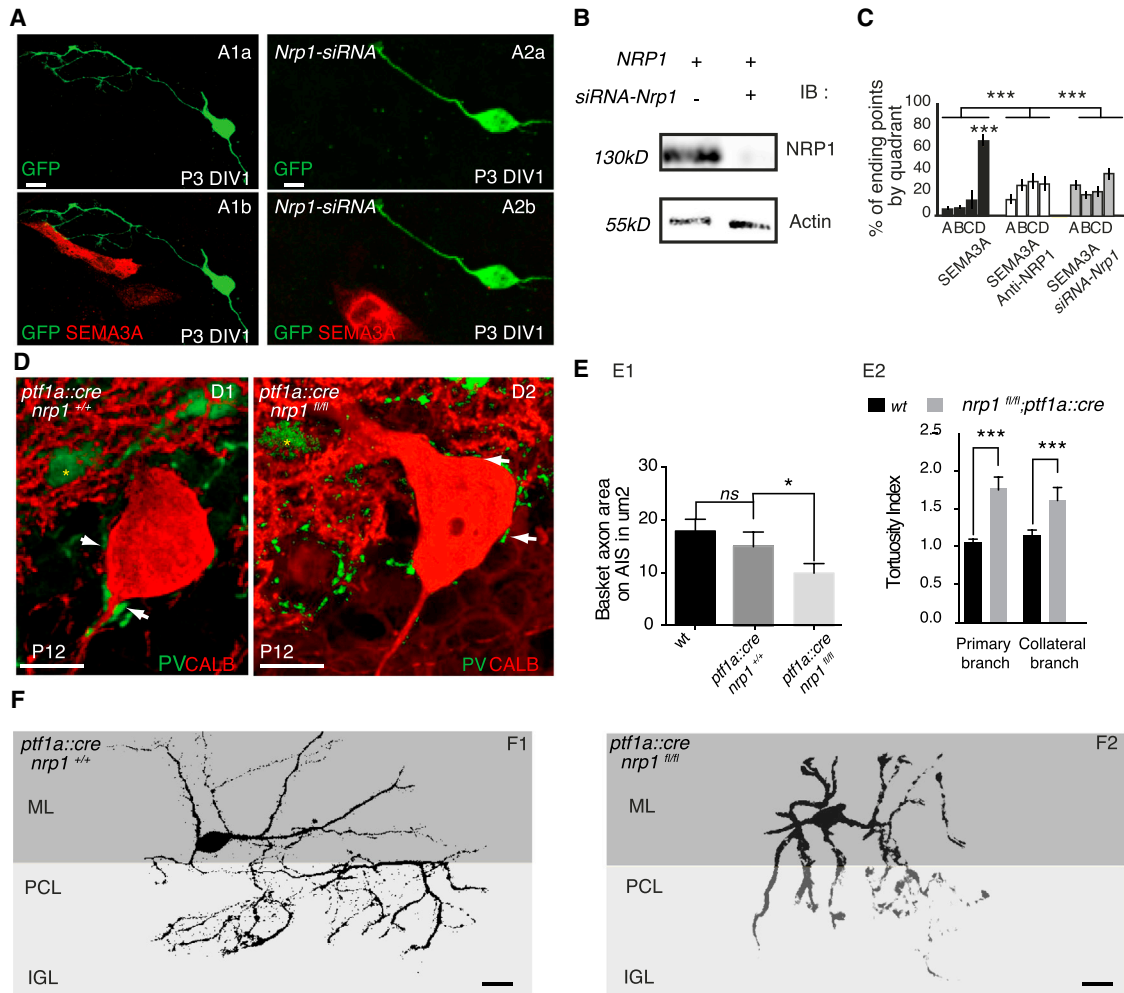


Figure 4. Specific Ablation of NRP1 in *ptf1a::cre; nrp1^{fl/fl}* Reproduces *sema3a^{-/-}* Phenotype

(A–C) Co-culture of GFP-labeled cerebellar interneurons mixed with CHO cells transfected with SEMA3A (red; A1 and A2) in presence (A2) or absence (A1) of an siRNA against *Nrp1*. Quantification showed a complete loss of the attraction effects of SEMA3A in the presence of *Nrp1*-siRNA (A2 and C; ****n* = 15, *p* < 0.00001, two-way ANOVA) or an antibody against NRP1 (C; ****n* = 20, *p* = 0.02, Student's *t* test). Western blot of HEK293 cells transfected with NRP1 in presence of *Nrp1*-siRNA confirmed a complete downregulation of the protein NRP1 (B).

(D–F) In vivo, BC axon organization was visualized with PARV staining (D) or Golgi staining (F) in both *ptf1a::cre; nrp1^{+/+}* (D1 and F1) and *ptf1a::cre; nrp1^{fl/fl}* (D2 and F2) at P12 (D) or P16 (F). Note that collateral position and tortuosity are totally aberrant in *ptf1a::cre; nrp1^{fl/fl}*, as in *sema3a^{-/-}* (F2; **n* = 10, *p* = 0.005, Student's *t* test). Quantification of pinceau area at the AIS of PCs in both *ptf1a::cre; nrp1^{+/+}* and *ptf1a::cre; nrp1^{fl/fl}* revealed a statistically significant decrease (E1; **n* = 19, *p* = 0.0183, Student's *t* test), together with increased axonal tortuosity (E2; ****n* = 10, *p* = 0.0002, Student's *t* test). Scale bars represent 10 μ m.

transfected with NF186 (Figure 6A2), but not with NRCAM (Figures 6A2 and 6C).

To further assess whether NRP1 can heterophyically interact with NF186, we transfected HEK293 cells with complementary DNAs encoding NRP1, NF186, or NRCAM, and then allowed them to aggregate (Figure 6B). We transfected these different cell populations separately with red (TOMATO) or GFP (Figure 6A). When HEK293 cells expressing NF186 (red) were plated in the presence of HEK293 cells expressing NRP1 (green), red and green cells co-aggregated to form mixed clusters (Figure 6B3), but when NRCAM was expressed instead of NF186, the transfected HEK293 cells did not aggregate (Figure 6B2). Moreover, NF186 and NRP1 proteins accumulated at sites of

contact between transfected cells (Figure 6B3), and when the B1B2 domains of NRP1 (NRP1 Δ B1B2) are deleted, this interaction is abolished (Figures 6B6 and 6D). Thus, NRP1-B1B2 domains were required for interaction of NRP1 with NF186 and cell-cell heterophilic adhesion. To firmly verify that endogenous NRP1 and NF186 belong to the same protein complex, we performed co-immunoprecipitation experiments. First, HEK293 cells were transfected with NF186 and WT NRP1, or NRP1 lacking A1A2 domains (NRP1 Δ A1A2) or NRP1 Δ B1B2. NF186 strongly co-precipitated with NRP1 and NRP1 Δ A1A2 (Figure 6E), but not with NRP1 Δ B1B2, thus reinforcing our observation from the cell aggregation assay (Figure 6B, quantified in Figure 6D). Furthermore, we investigated the likelihood of this interaction

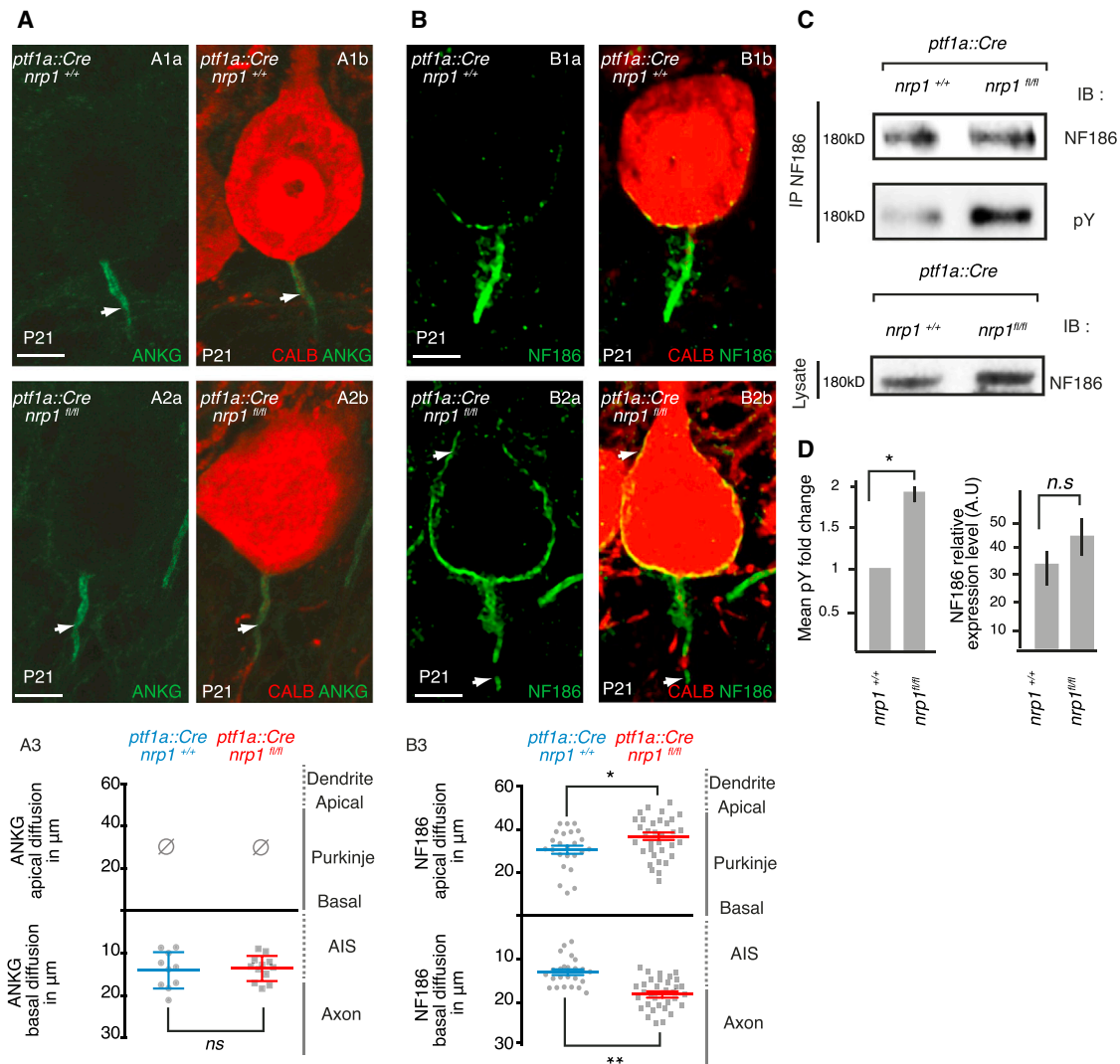


Figure 5. NF186, but Not ANKG, Expression Is Diffused in *ptf1a::cre; nrp1^{fl/fl}*

(A and B) Expression of ANKG by PCs at P21 (green; A) and NF186 (green; B) in both *ptf1a::cre; nrp1^{+/+}* (A1 and B1) and *ptf1a::cre; nrp1^{fl/fl}* (A2 and B2). PCs are labeled with CALB (red; A and B). Scale bars represent 5 μm . Quantification of ANKG localization in *ptf1a::cre; nrp1^{fl/fl}* showed no significant difference for basal and apical diffusion (A3; ns, $n = 14$, $p = 0.77$, Student's t test) in PCs compared to *ptf1a::cre; nrp1^{+/+}* (A1 and A2), in contrast to NF186 (B1 and B2), which showed a clear significant difference for basal (B3; ** $n = 34$, $p = 0.0017$, Student's t test) and apical diffusion (B3; * $n = 34$, $p = 0.012$, Student's t test). (C and D) Immunoprecipitation of NF186 shows that phospho-tyrosine (PY) is increased in *ptf1a::cre; nrp1^{fl/fl}* (C), as quantified in (D) ($n = 3$, $p = 0.006$, Student's t test).

in vivo using specific anti-NRP1 and anti-NF186 antibodies (Figure 6F) and observed a strong alignment of both proteins at the AIS of PCs (Figure 6F3). Finally, we could co-immunoprecipitate NRP1 with NF186 from WT, but not from *ptf1a::cre; nrp1^{fl/fl}*, mouse cerebellar cortex (Figure 6G). Thus, NRP1 heterophilic recognition and interaction with the extracellular domain of NF186 are likely to be involved in PC AIS target innervation.

Because NF186 is expressed in both pre- and postsynaptic sites in cerebellum (Buttermore et al., 2012), we investigated whether NRP1 and NF186 could interact in cis by co-capping experiments (Wong et al., 2000). Specific antibody for NRP1 was used to cross-link NRP1 on the surface of NF186-expressing

HEK293 cells. Formation of NRP1 caps was observed as a cluster of fluorescent spots on the cell surface (Figure 6H). NF186 expression was detected on the same cells by indirect immunofluorescence staining with NF186 polyclonal antibodies and showed that NF186 did not co-localize with NRP1 (Figures 6H1 and 6H2), suggesting that these proteins were not associated in cis within the plasma membrane. In contrast, when the co-capping was performed with L1CAM or Plexin A1, known binding partners of NRP1, clusters of L1CAM and Plexin A1 co-localized with NRP1 caps, confirming their association in cis (Figures 6H3 and 6H4). Thus, our data showed that NRP1 and NF186 were associated in trans, but not in cis.

SEMA3A and NF186 Expression Are Both Required for BC Axon Subcellular Target Recognition

Since in our *in vitro* cell aggregation assay SEMA3A is dispensable for NF186/NRP1 interaction, we therefore investigated if axon guidance mediated by SEMA3A was necessary to induce cell recognition in our co-culture model. *gad67::gfp* interneurons were plated on a high percentage of CHO cells expressing NF186 alone. The logic was that GABAergic axons will likely encounter NF186-expressing cells, although they will not be guided by SEMA3A. In this condition, axons of GABAergic interneurons did not show specific interaction with NF186-expressing CHO cells as compared to CHO cells expressing TOMATO (Figure S7). In contrast, when NF186 was co-expressed with SEMA3A, we found that GABAergic axons wrapped CHO cells co-expressing SEMA3A and NF186 (Figure 7A3; **** $n = 24$, $p = 0.0001$, Fisher's test), but not cells co-expressing SEMA3A and NRCAM (Figures 7A4 and 7C; arrows, ns, $n = 15$, $p = 0.68$, Fisher's test). Thus, our data showed that SEMA3A and NF186 acted together to specify BC axon layout and target recognition.

To further confirm that both NF186 and SEMA3A were necessary for BC axon target recognition and innervation, we explored this possibility in our heterologous cell graft assay. CHO cells co-expressing NF186 and SEMA3A were injected in the cerebellum, and BC axon localization was assessed. In contrast to BC axon retraction observed in the presence of SEMA3A-expressing CHO cells (Figure 2H4) or lack of BC axons in the presence of NF186-expressing CHO cells (Figures 7B1a–7B1c and 7C; ns, $n = 9$, $p = 1$, Fisher's test), BC misrouted axons stayed in GCL around the CHO cells expressing both NF186 and SEMA3A for a longer time period (Figures 7B2a–7B2c and 7D; $n = 13$, $p = 0.0210$, Fisher's test). Altogether, these results showed that expression of NF186 together with SEMA3A was sufficient to prevent BC axon retraction and to promote target recognition and innervation.

Local SEMA3A Promotes NRP1 Expression at the Axonal Cell Surface

How could we resolve the apparent discrepancy of the requirement of SEMA3A in BC axon recognition of NF186-expressing cells and SEMA3A's unneeded role in mediating *trans*-interaction between NRP1 and NF186 *in vitro*? To investigate this question, we hypothesized that local SEMA3A stabilized NRP1 expression at the cell surface to trigger interaction with NF186. Indeed, secreted SEMA3A anchored at the cell surface through its C-terminal domain could locally stabilize NRP1 (Figure S1) (De Wit et al., 2005, 2009). Thus, we labeled NRP1 in the presence or absence of SEMA3A in non-permeabilized conditions. Cell-surface clusters of NRP1 were observed in the presence of SEMA3A-expressing CHO cells, but not in control condition or when CHO cells expressed NF186 alone (Figures 8A–8C). Clusters of NRP1 along the interneuron axon co-localized with SEMA3A expressed by CHO cells (Figure 8B). These results show that local SEMA3A stabilized NRP1 expression at neuronal cell surface. In addition, we observed the formation of NF186 clusters only in the presence of SEMA3A that co-localized with SEMA3A along the interneuron axon (Figures 8D and 8E). Therefore, NRP1 surface expression stabilized by local SEMA3A could facilitate its *trans*-interaction with NF186.

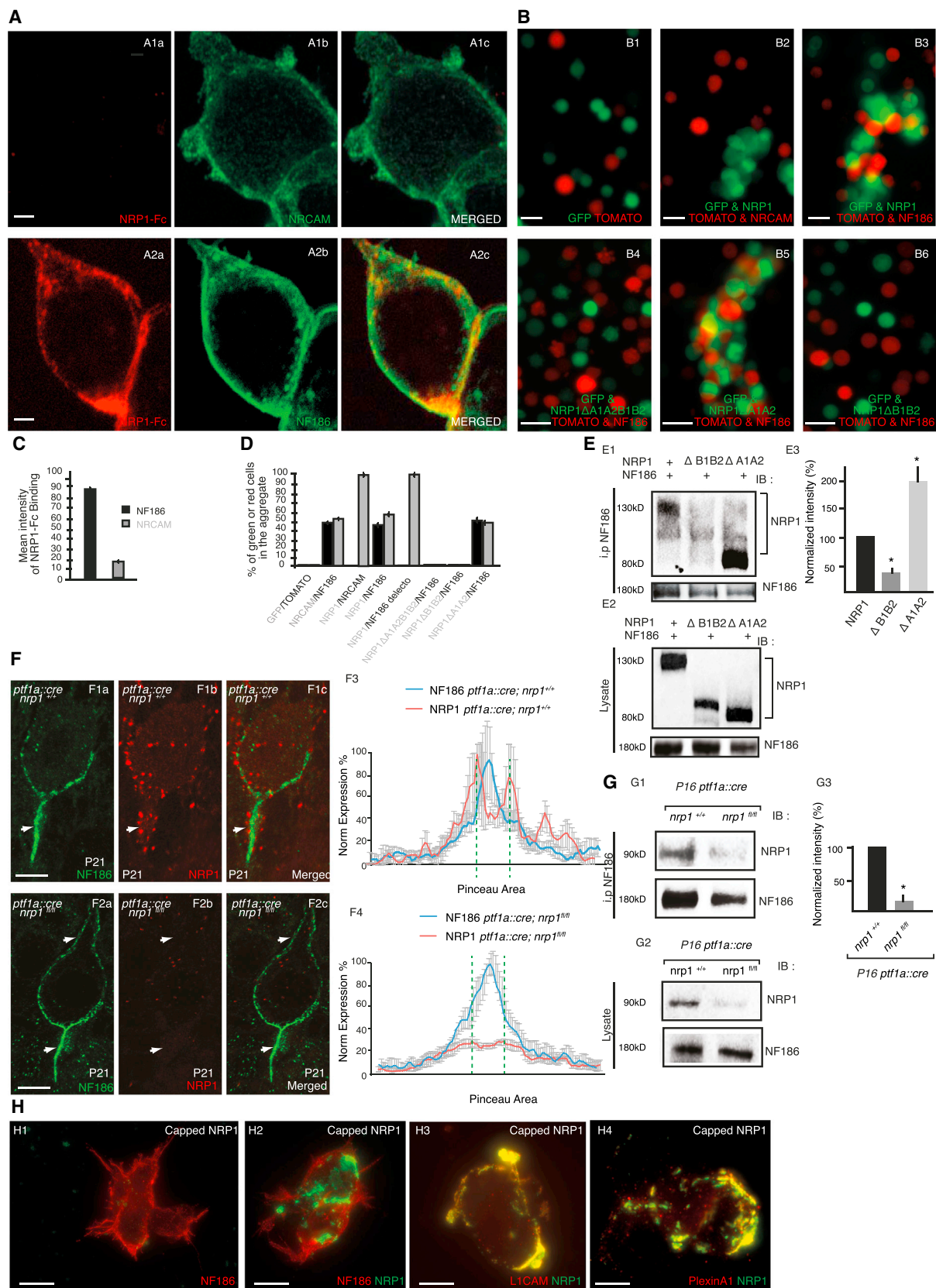
To better pinpoint the molecular interplay among NRP1, SEMA3A, and NF186, we next asked whether NRP1 binding to SEMA3A or NF186 was mutually exclusive. SEMA3A binding to NRP1 depended mostly on A1A2 domains of NRP1 (Janssen et al., 2012). In our study, we showed that NRP1 lacking A1A2 domains (NRP1 Δ A1A2) interacted with NF186 in our cell aggregation assay and also by co-immunoprecipitation *in vitro* (Figure 6), suggesting that SEMA3A binding and NRP1/NF186 interactions were on different sites. To strengthen this observation, we performed a neuropilin-Fc binding assay on cells expressing NF186 alone or in the presence of SEMA3A. We observed that NRP1-Fc bound to NF186 in both conditions (Figures 8F and 8G). Moreover, co-localization of the three partners within the same clusters showed that binding of NRP1 to both SEMA3A and NF186 happened at the same time and was not mutually exclusive (Figure 8G). Altogether, our data demonstrated that NRP1 stabilization at the cell surface by local SEMA3A promoted NRP1 *trans*-interaction with NF186 and therefore favored target innervation (Figure 8H).

DISCUSSION

The construction of local GABAergic circuits is an important process during CNS development that involves precise cellular and subcellular target innervation to fulfill physiological neuronal network synaptic function (Porter et al., 2001; Tamás et al., 2003). Our findings provide new insights into the molecular mechanisms responsible for synaptic specificity during construction of neuronal circuits. As a model, we studied GABAergic innervation of PCs by BCs and demonstrate that the long-range axon guidance molecule SEMA3A and its binding receptor NRP1 are sufficient to attract the axon of the GABAergic interneuron at the AIS of PCs. Subsequently, NRP1 is engaged in target recognition and contact stabilization through *trans*-interaction with the postsynaptic protein NF186, thus participating in the construction of the PC pinceau. This provides a striking example of a local molecular continuum mechanism between guidance and adhesion/recognition functions in the construction of neuronal circuitry.

Specific Local GABAergic Circuit Formation by Guidance Cues

Here, we provide evidence that shows precise guidance of local GABAergic interneuron axons is occurring through extracellular cues, even though BCs are physically close to PCs. We observed that local expression of SEMA3A was sufficient to attract BC axons toward their targets, both *in vitro* and *in vivo*, in an NRP1-dependent manner. This finding shows that BC axon geometric specificity is shaped by local external cues. This is in line with the observation that GABAergic axon trajectories are well correlated with their postsynaptic targets as opposed to the rather straight axons of projecting neurons that made en passant synapses with nearby targets (Stepanyants et al., 2004). Compelling evidence of the role of SEMA3A in BC axon organization and guidance was obtained by ectopic expression of SEMA3A *in vivo*, which induced aberrant axonal pathfinding. This aberrant axonal targeting is also observed when PCs are misplaced in GCL, as is the case in the cerebellar-deficient folia



(legend on next page)

(alpha N-catenin) mutant mice. These data suggest an instructive role of SEMA3A in target cells for local axonal pathfinding of GABAergic interneurons.

Once GABAergic axons reach their target field, they contact postsynaptic cells using molecular cues that remain poorly understood. For example, in the cortex nearly all pyramidal cells receive inhibitory inputs from different types of GABAergic interneurons without noticeable discrepancy, arguing for a rather unspecific innervation mechanism (Lee et al., 2006; Packer and Yuste, 2011; Wierenga et al., 2008). On the other hand, specificity and stringency of GABAergic connectivity have been demonstrated (Ango et al., 2004; Betley et al., 2009; Stepanyants et al., 2004). Both mechanisms may not be mutually exclusive, as dense local connectivity is not necessary random and could be instructed by specific target recognition mechanisms. Here, we observed that ectopic expression of SEMA3A alone only induced transient aberrant axonal localization. Although many potential targets are present in the cerebellar GCL, axons of BCs retracted during cerebellar development. Our result is reminiscent of the observation in spinal cord, where GABAergic neurons do not form connections with other available local neurons, and instead retract their axons, arguing for high stringency in the recognition program (Betley et al., 2009).

Role of NF186 in Axon Pathfinding

We and others have previously shown that NF186 expressed by PCs was necessary to stabilize pinceau synapses (Ango et al., 2004; Kriebel et al., 2011; Zonta et al., 2011). Recent data further suggested that NF186 might be involved in guiding BC axons (Buttermore et al., 2012). In fact, knocking down NF186 in BCs and/or PCs disrupted the stereotyped organization of BC axon collaterals in the ML (Buttermore et al., 2012). Here, we provide evidence that NF186 alone was not sufficient to attract BC axons. We observed that both in vitro and in vivo expression of NF186 had no effect on BC axon localization per se. Instead, we found that PCs secrete SEMA3A, which accumulates around the soma and attracts GABAergic axons toward the PCL (Carulli et al., 2013; Cioni et al., 2013). But how do we reconcile the NF186 knockdown phenotype with SEMA3A function on BC

axon organization? Accumulating evidence suggests that the L1CAM family is involved in regulating SEMA3A function by forming a ternary complex with the classical SEMA3A receptor composed of NRP1 and Plexin As (Castellani et al., 2000; Wright et al., 2007). It is then possible that NF186 belongs to the SEMA3A receptor complex, as demonstrated for other L1CAM family members such as L1, CHL1, and NRCAM (Castellani et al., 2000; Demyanenko et al., 2011; Wright et al., 2007). However, we were unable to identify *cis*-interaction between NF186 and NRP1. Alternatively, NF186 may affect sensitivity of GABAergic axons to SEMA3A by regulating the trafficking of SEMA3A receptor complex (Dang et al., 2012; Law et al., 2008). Indeed, during axonal navigation SEMA3A-induced growth cone remodeling is correlated with endocytosis of NRP1 (Betley et al., 2009; Castellani et al., 2004; Fournier et al., 2000). Interestingly, NRP1 internalization is controlled by L1CAM (Castellani et al., 2002) and hence provides an entry point for NF186 to control axon guidance. Indeed, NF186 expressed in BC axons (Buttermore et al., 2012) could control NRP1 internalization during axon navigation indirectly through interaction with TAG-1 (Volkmer et al., 1998), a protein that was recently shown to control NRP1 endocytosis (Dang et al., 2012). The observation that specific deletion of NF186 in both PC and BC axons, but not in PCs solely (Buttermore et al., 2012), induced BC axon disorganization favors the hypothesis of a presynaptic action of NF186.

Local Molecular Continuum between Axon Guidance and Cell Recognition

One important result of our study is that NRP1 provides a molecular bridge between guidance and target recognition, which ensures precise subcellular innervation of PCs by BC axons. The prevailing view of target recognition is that a specific set of recognition molecules such as CAMs are expressed locally in discrete cell populations and at specific subcellular domains. Nevertheless, the mechanism that ensures the final encounter between pre- and postsynaptic elements in a micrometer range remains unknown. For example, in the retina pre- and postsynaptic cells expressing the same adhesion molecule are

Figure 6. NF186 *trans*-Interacts with NRP1 via its B1B2 Domain

(A and C) Soluble NRP1-Fc (red; A) interacts specifically with HEK293 cells transfected with NF186 (green; A2), but not with another L1CAM family molecule, NRCAM (green, A1).

(B) Aggregation assay of mixed HEK293 cells transfected with GFP or TOMATO alone (B1) showed no intrinsic adhesion properties. When cells are transfected with NRP1 and GFP (B2) and further mixed with cells transfected with NRCAM and TOMATO (B2), we detected a clear *trans*-homophilic adhesion for NRP1-NRP1 (green aggregate), but no heterophilic adhesion with NRCAM- and TOMATO-expressing cells (B2). In contrast, when NRP1- and GFP (B3)-transfected cells are mixed with NF186 and TOMATO cells (B3), we observed a strong heterophilic *trans*-interaction. Moreover, we completely lost this *trans*-interaction when NRP1 is truncated for its B1B2 domains (B4 and B6), but not when A1A2 are deleted (B5).

(C) Quantification of (A).

(D) All quantifications of the cell aggregation assay in (B).

(E) NRP1 and NF186 co-immunoprecipitated in vitro, and this interaction is completely lost when the NRP1-B1B2 domains are absent (E1 and E2). Co-immunoprecipitation intensity was normalized to NF186 immunoprecipitation (E3) ($n = 3$, $*p = 0.02$, Student's *t* test).

(F) A PLA assay at P21 for NRP1 co-labeled with NF186 in both *ptf1a::cre; nrp1^{+/+}* (F1) and *ptf1a::cre; nrp1^{fl/fl}* (F2). Note the strong proximity between NF186 and NRP1 (arrows; F1), as quantified in (F3). In *ptf1a::cre; nrp1^{fl/fl}*, we completely lost NRP1 expression around PCs. Moreover, NF186 diffused along PC apical membrane and AIS (arrows; F2).

(G) In vivo, NRP1 and NF186 co-immunoprecipitated strongly in *ptf1a::cre; nrp1^{+/+}*, and we specifically lost this interaction in *ptf1a::cre; nrp1^{fl/fl}* (G1 and G2), as quantified in (G3). A co-capping assay was performed with NRP1.

(H) Capping of NRP1 was induced in control cells expressing NF186 alone (H1) or cells expressing NRP1 with NF186 (H2), L1CAM (H3), or Plexin A1 (H4).

Scale bars represent 10 μm .

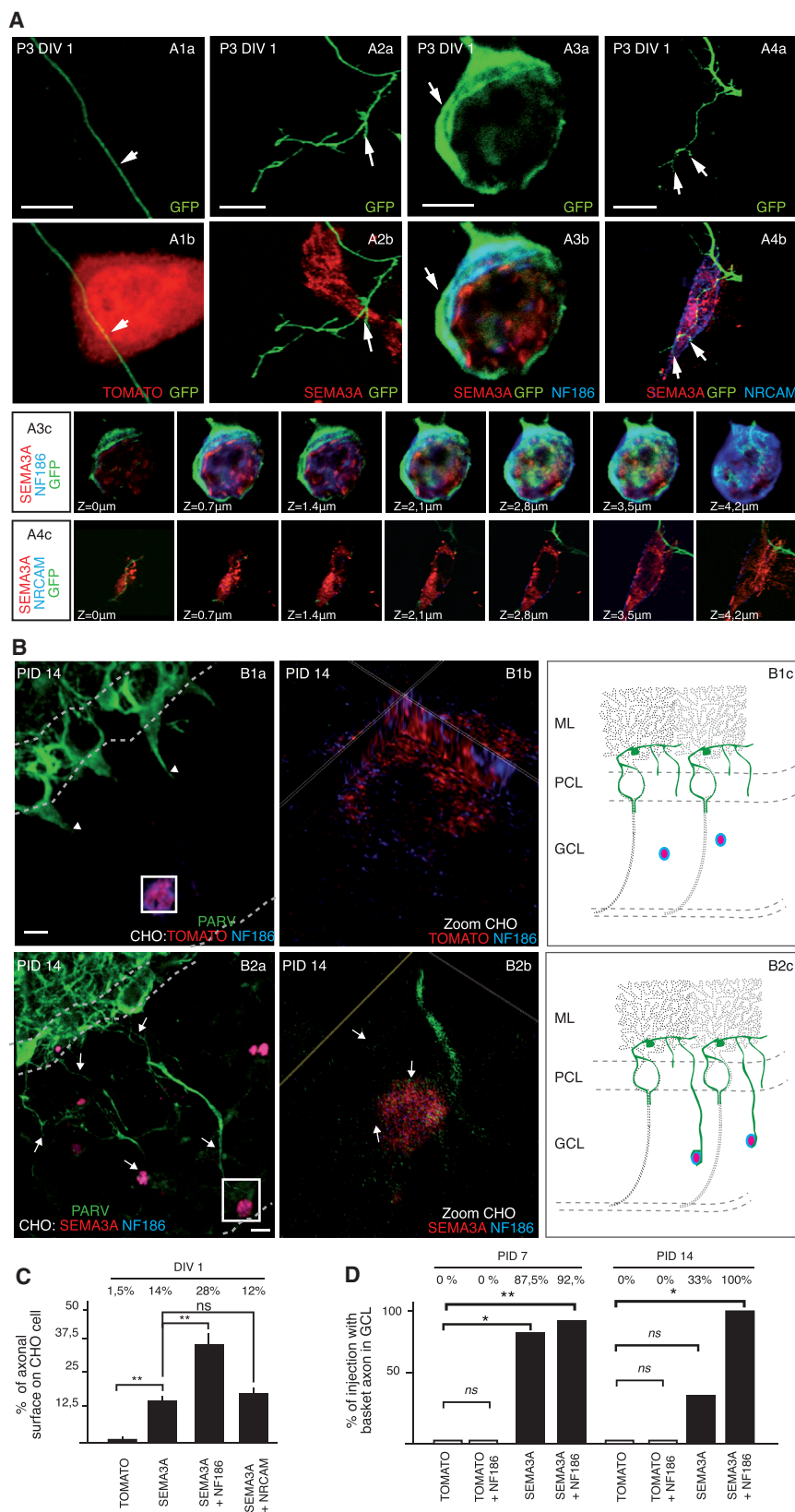


Figure 7. SEMA3A and NF186 Act Together to Stabilize BC Axons In Vitro and In Vivo

(A) Co-culture of GFP-positive interneurons mixed with CHO cells transfected with control TOMATO (red; A1), SEMA3A (red; A2), SEMA3A and NF186 (red and blue, respectively; A3) or SEMA3A and NRCAM (red and blue, respectively; A4). Note that only co-expression of SEMA3A with NF186 triggers a near-complete coverage of the CHO cells with GFP-positive axons (arrow; A3). High magnification in (A3c) and (A4c) showed across Z stack how the axon enwrapped the CHO cells in SEMA3A co-expressed with NF186 (A3c), but not with NRCAM (A4c), as analyzed in (C).

(B) Cerebellar grafts of CHO cells expressing NF186 and TOMATO have no intrinsic effects on BC axon attraction in GCL (B1). Note the characteristic pinneau formation on the PCs (arrows; B1a); summarized in (B1c). However when SEMA3A was co-expressed with NF186 (B2), we clearly observed a strong and significant increase of ectopic BC axons in GCL at P7 and up to PID 14 (arrow; B2b); summarized in (B2c).

(C) Quantification of percent of axonal surface coverage on CHO cells. Co-expression of SEMA3A with NF186 induced significant axon surface coverage of the CHO cells (** $n = 24$, $p = 0.0001$, Fisher's test). However, co-expression of SEMA3A with NRCAM failed to induce coverage of the CHO cells with GFP-positive axons (arrow; A4 and C; ns , $n = 15$, $p = 0.68$, Fisher's test).

(D) Quantification of ectopic BC axons in the GCL. TOMATO- or NF186-expressing CHO cells failed to attract basket axon in the GCL (ns , $n = 9$, $p = 1$, Fisher's test). However, when SEMA3A was co-expressed with NF186, we clearly observed a strong and significant increase of ectopic BC axons in GCL at P7 (** $n = 20$, $p < 0.001$, Fisher's test) and up to PID 14 (* $n = 13$, $p = 0.0210$, Fisher's test).

Scale bars represent 10 μ m.

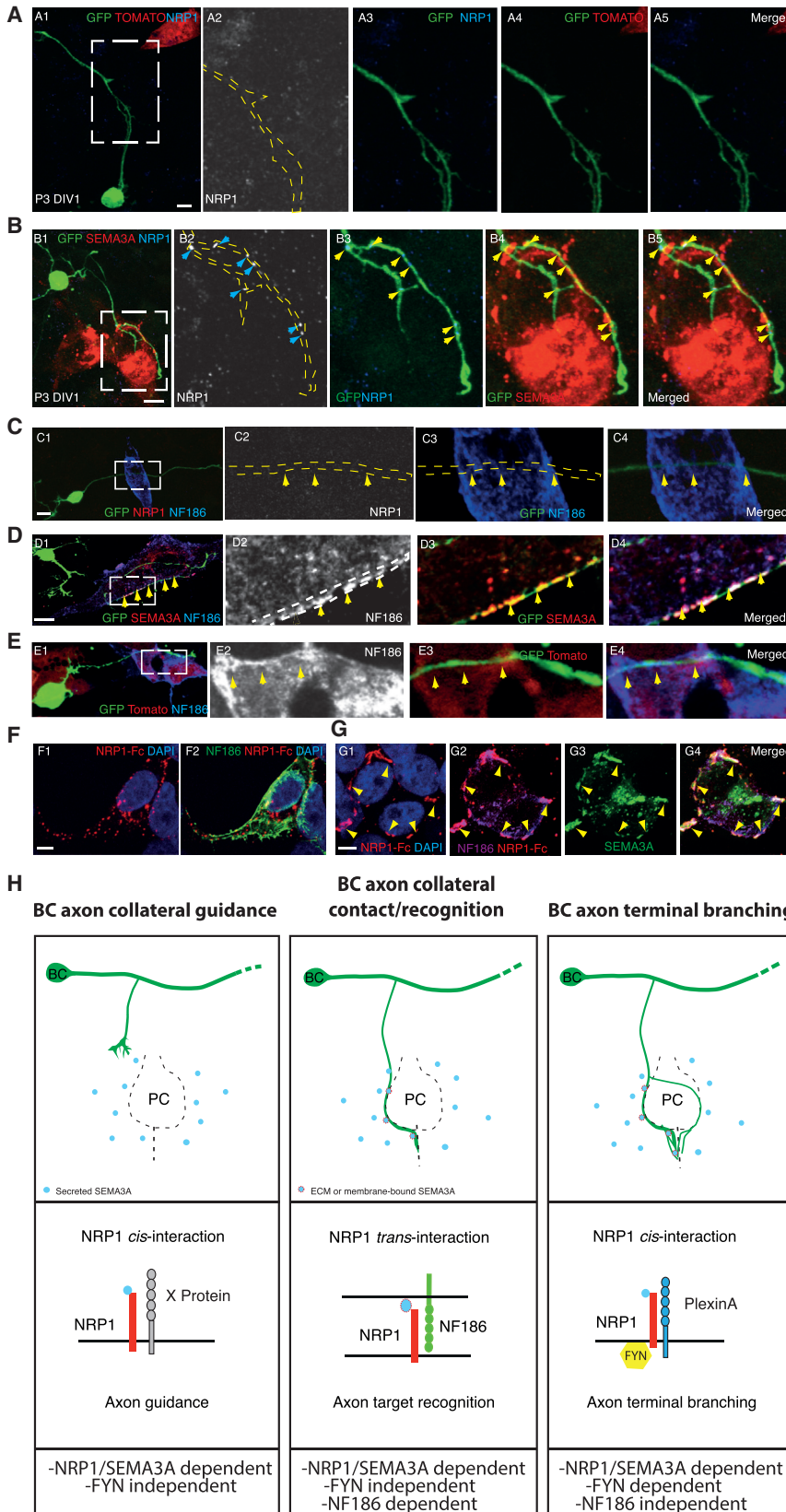


Figure 8. SEMA3A Stabilizes NRP1 at Axonal Cell Surface and Facilitates NF186 Binding

(A–C) Co-culture of GABAergic interneurons with CHO cells expressing TOMATO (A), SEMA3A-TOMATO (B), or SEMA3A-TOMATO with NF186 (C). In non-permeabilized condition (A1–A5), NRP1 labeling is not detectable at the cell surface (A2). In the presence of SEMA3A-TOMATO (B1–B5), NRP1 (B2) is present at the axonal cell surface at points of contact with SEMA3A. Blue arrows in (B2) indicate NRP1 labeling. Yellow arrows highlight the co-localization of NRP1 with SEMA3A. In the presence of NF186 alone (C1–C4), no NRP1 expression was observed at point of contact with BC axons (yellow arrows).

(D) When CHO cells co-expressed SEMA3A-TOMATO and NF186, NF186 co-localized with SEMA3A-TOMATO puncta (yellow arrows) at contact points with BC axons (D3 and D4). Dashed lines in (A)–(D) outline GABAergic axon localization.

(E) Note that NF186 expression alone does not form puncta at contact points with BC axons (yellow arrowheads; E1–E4). Scale bars represent 10 μ m.

(F) Soluble NRP1-Fc (red; F1) interacted specifically with HEK293 cells transfected with NF186 (green; F2).

(G) In the presence of SEMA3A (green; G3 and G4), soluble NRP1-Fc (red; G1, G2, and G4) still interacted with NF186 (purple; G2 and G4). Note that NRP1-Fc co-localized with SEMA3A and NF186 (yellow arrowheads).

(H) Model depicting the dual NRP1 functions in BC axon pathfinding (left panel), subcellular recognition (middle panel), and terminal branching (right panel). During axonal navigation, NRP1 expressed in BC axons (red rectangle) is guided by secreted SEMA3A (blue circle, left panels). *cis*-interaction of NRP1 with protein X regulates axon guidance. As BC axons reach their target area, extracellular matrix (ECM)-attached or membrane-bound SEMA3A (blue circle with red border) stabilized NRP1 at BC membrane (middle panel) and facilitated BC axon target recognition through NF186 *trans*-interaction. NRP1 switches from *cis*-interaction with SEMA3A to *trans*-interaction with NF186 (middle panels) to mediate adhesion/recognition. Finally, BC axons at PC AIS will form extensive terminal branching in an SEMA3A-FYN-dependent manner (left panel).

organized into the same sublaminae and form synaptic contacts through homophilic interactions. Interestingly, forced expression of a new adhesion protein in this model triggers mistargeting of neuritic processes to a new sublamina (Yamagata and Sanes, 2008). Although the mechanism that guides both neuritic processes in specific sublaminae is not understood, the result is supportive of the idea that axon guidance and target recognition are intimately linked.

Here we demonstrated that NRP1 involved in BC axon guidance is subsequently engaged in target recognition by *trans*-interacting with NF186 located at PC AIS. The adhesion property of NRP1 was discovered long before its role in axon guidance (Takagi et al., 1995), but until now the binding elements of NRP1 that mediate this function were unknown. Our data show that B1B2 domains of NRP1 are involved in the interaction with NF186. The same domains were also identified previously to mediate cell adhesion function in heterologous cell lines (Shimizu et al., 2000; Takagi et al., 1995). How is NRP1 engaged in axon guidance switch to cell adhesion activity? Axon guidance molecules SEMA3s and Plexin As do not interact with B1B2 domains of NRP1 (Shimizu et al., 2000), suggesting that the dual functions of NRP1 may occur independently. However, we cannot exclude the possibility that the adhesion activity of NRP1 could inhibit its axon guidance function and vice versa. One intriguing observation is that NRP1 functions depend on the mode of interaction with L1CAM. It has been proposed that *trans*-interaction of NRP1 with L1CAM can switch NRP1 function induced by *cis*-interaction (Castellani et al., 2002). It is therefore tempting to speculate that switching NRP1 binding mode ensures the transition from guidance to adhesion by facilitating target cell recognition, possibly via specific structural domains (Figure 8H).

Overwhelming evidence suggests that many molecules that were initially discovered for their functions in axon guidance also play important functions in synapse formation, as reviewed in Chen and Cheng (2009). Although these steps can certainly happen independently, our results provide proof of the existence of a molecular link between these steps that may facilitate the task of matching appropriate pre- and postsynaptic partners. Future studies combining both properties of these molecules might shed further light on the rules that govern formation of brain connectivity.

EXPERIMENTAL PROCEDURES

Mixed Co-culture Assay

Animals and surgical procedures are described in the [Supplemental Experimental Procedures](#). The experimental plan was designed according to the European Communities Council Directive and the French law for care and use of experimental animals with authorization number B 34-309 and approved protocol number CEEA-LR-1103.

CHO cells were maintained in Ham F12 (GIBCO) supplemented with 10% fetal calf serum and a mix of penicillin/streptomycin. A total of 15×10^4 cells were plated in a 24-well plate containing 18 mm coverslips and coated with Poly-L-Ornithine. After 1 day, cells were transfected with plasmids using JetPrime transfection reagent (PolyPlus) for 15 hr. The medium was then replaced with fresh Neurobasal supplemented with Glutamax (GIBCO), B27 (GIBCO), and a mix of penicillin/streptomycin. At the same time, dissociated cerebellar GABAergic interneurons were plated on CHO cells (10^5 cells/well). We plated neurons at low density to allow analysis of individual cells.

In Vivo Injection of CHO Cells

CHO cells were maintained in Ham F12 supplemented with 10% fetal calf serum and a mix of penicillin/streptomycin. A total of 1×10^6 cells were plated in 10 cm dishes. After 1 day, cells were transfected with plasmids using the JetPrime transfection reagent (PolyPlus) for 15 hr. The next day, cells were trypsinized (Trypsin 0.25%, GIBCO) and diluted to a concentration of 5,000 cells/ μ L. The same day, P8 pups were anesthetized as previously described. After incision of the skin overlying the skull, a small hole was made directly over the left hemisphere of the cerebellum by trepanation. A micropipette was inserted to a depth of 1.5 mm below the skull to inject 2 μ L cell suspension.

Analysis of CHO Grafting

Seven or 12 days after CHO grafting, cerebellar slices that contained CHO cells were imaged using confocal microscopy. CHO cells expressing our transgene were systematically imaged using the red and green channels. After acquisition, all images were analyzed using ImageJ. Pixel intensity in the green channel, corresponding to BC axon immunofluorescence, was measured, including 40 μ m around the CHO cells. The same region of interest (ROI) was used in all images.

Histological Procedures, Immunohistochemistry, PLA, Golgi Staining, and Fc Binding

Under deep general anesthesia, experimental animals were transcardially perfused with 4% paraformaldehyde in 0.12 M phosphate buffer (pH 7.2–7.4) (10 mL). Brains were immediately dissected and stored overnight in the same fixative at 4°C. Cerebella were then cut with a vibratome in 70 μ m parasagittal sections collected in PBS. Sections obtained from different experimental sets were processed for immunofluorescent labeling with different primary antibodies after 2 hr in a blocking solution containing PBS, 0.2% Triton X-100, and 5% horse serum. For mixed co-culture assay, after 24 hr of growth, cultures were fixed with 4% paraformaldehyde in PBS, permeabilized with 0.2% Triton X-100, and immunostained.

For Fc binding experiments, rat NRP1-Fc (5 μ g/mL) from R&D Systems was applied to the culture medium for 1 hr and then incubated with fluorescein-conjugated and anti-human Fc (1:200) prior to fixation in 4% paraformaldehyde. NF186 is then processed using classical immunohistochemistry.

For the PLA technique, 60 μ m sagittal sections were treated for NRP1 immunolabeling before application of Goat Plus and Minus probes. Experiments were then done according to the manufacturer's instructions (Olink Bioscience).

For Golgi staining, fixed cerebellum 250- μ m-thick slices were immersed in impregnation solution (Bioenno Tech, LLC) for 5 days in the dark, followed by incubation in the staining solution (Bioenno Tech, LLC) to develop the impregnation. Finally, slices were dehydrated in graded ethanol baths, cleared in xylene, and mounted on slides with Permount mounting medium.

Co-capping Assay

To cap surface NRP1, cells were incubated with anti-NRP1 antibody (1/500, in HBSS, 1% horse serum) for 30 min at 4°C. Cells were washed in ice-cold HBSS and labeled with Alexa488 secondary antibody (1/100, in HBSS, 1% horse serum). Cells were incubated for 1 hr at 37°C and then fixed with 4% paraformaldehyde for 15 min. Detection of NF186, L1CAM, or Plexin A1 was performed at room temperature with dedicated primary and secondary antibodies. Finally, cells were washed, mounted in Vectashield, and imaged using a ZEISS LSM780 confocal microscope.

Aggregation Assay

HEK293T cells were maintained in DMEM supplemented with 10% fetal calf serum and a mix of penicillin/streptomycin. A total of 1×10^5 cells were plated in 3 cm dishes. After 1 day, cells were transfected with plasmids of interest associated with GFP or TOMATO, depending on the experimental condition, using the JetPrime transfection reagent (PolyPlus) for 15 hr. The next day, cells were trypsinized (Trypsin 0.25%, GIBCO) and resuspended in 1 mL DMEM. Cells were then mixed together and plated for 2 hr at room temperature in a 1:1 ratio (GFP and TOMATO).

SUPPLEMENTAL INFORMATION

Supplemental Information includes Supplemental Experimental Procedures and seven figures and can be found with this article online at <http://dx.doi.org/10.1016/j.neuron.2016.08.015>.

AUTHOR CONTRIBUTIONS

F.A. and L.T. conceived the project; L.T. and C.C. performed the experiments. J.-M.C. and V.S. participated in experiments and performed gene expression analysis. C.J.-T., R.E.H., C.S.-F., A.D., and A.B.H. assisted with experiments and provided critical materials. F.A., L.T., and C.C. wrote the manuscript with contributions from all authors.

ACKNOWLEDGMENTS

Sema3a-gfp clone and pBluescriptII-KS-*semaIII* were kind gifts of Dr. J. Verhaagen (CNCR) and Dr. A. Chédotal (Institut de la vision), respectively. NF186 plasmid was provided by Dr. V. Bennett (University of North Carolina). We also thank M. Niquille for experimental help. F.A. was supported by Human Frontier Science Program Organization (CDA-0015-2006-C) and INSERM-AVENIR program. F.A. has support from Fondation Fyssen, Fédération pour la recherche sur le cerveau (FRC), Fondation pour la recherche Médicale (FRM), and ANR (ANR-08-JCJC-0044). We would like to thank Isabelle Bachy for *Sema3A* in situ hybridization and Joël Bockaert, Laurent Fagni, and Denis Jabaudon for critical reading of the manuscript.

Received: March 13, 2015

Revised: February 5, 2016

Accepted: July 30, 2016

Published: September 8, 2016

REFERENCES

- Ango, F., di Cristo, G., Higashiyama, H., Bennett, V., Wu, P., and Huang, Z.J. (2004). Ankyrin-based subcellular gradient of neurofascin, an immunoglobulin family protein, directs GABAergic innervation at Purkinje axon initial segment. *Cell* 119, 257–272.
- Ango, F., Wu, C., Van der Want, J.J., Wu, P., Schachner, M., and Huang, Z.J. (2008). Bergmann glia and the recognition molecule CHL1 organize GABAergic axons and direct innervation of Purkinje cell dendrites. *PLoS Biol.* 6, e103.
- Betley, J.N., Wright, C.V., Kawaguchi, Y., Erdélyi, F., Szabó, G., Jessell, T.M., and Kaltschmidt, J.A. (2009). Stringent specificity in the construction of a GABAergic presynaptic inhibitory circuit. *Cell* 139, 161–174.
- Biederer, T., and Scheiffele, P. (2007). Mixed-culture assays for analyzing neuronal synapse formation. *Nat. Protoc.* 2, 670–676.
- Buttermore, E.D., Piochon, C., Wallace, M.L., Philpot, B.D., Hansel, C., and Bhat, M.A. (2012). Pinceau organization in the cerebellum requires distinct functions of neurofascin in Purkinje and basket neurons during postnatal development. *J. Neurosci.* 32, 4724–4742.
- Carulli, D., Foscarin, S., Faralli, A., Pajaj, E., and Rossi, F. (2013). Modulation of semaphorin3A in perineuronal nets during structural plasticity in the adult cerebellum. *Mol. Cell. Neurosci.* 57, 10–22.
- Castellani, V., Chédotal, A., Schachner, M., Favre-Sarrailh, C., and Rougon, G. (2000). Analysis of the L1-deficient mouse phenotype reveals cross-talk between *Sema3A* and L1 signaling pathways in axonal guidance. *Neuron* 27, 237–249.
- Castellani, V., De Angelis, E., Kenrick, S., and Rougon, G. (2002). Cis and trans interactions of L1 with neuropilin-1 control axonal responses to semaphorin 3A. *EMBO J.* 21, 6348–6357.
- Castellani, V., Falk, J., and Rougon, G. (2004). Semaphorin3A-induced receptor endocytosis during axon guidance responses is mediated by L1 CAM. *Mol. Cell. Neurosci.* 26, 89–100.
- Chen, S.Y., and Cheng, H.J. (2009). Functions of axon guidance molecules in synapse formation. *Curr. Opin. Neurobiol.* 19, 471–478.
- Cioni, J.M., Telley, L., Saywell, V., Cadilhac, C., Jourdan, C., Huber, A.B., Huang, J.Z., Jahannault-Talignani, C., and Ango, F. (2013). *SEMA3A* signaling controls layer-specific interneuron branching in the cerebellum. *Curr. Biol.* 23, 850–861.
- Dang, P., Smythe, E., and Furley, A.J. (2012). TAG1 regulates the endocytic trafficking and signaling of the semaphorin3A receptor complex. *J. Neurosci.* 32, 10370–10382.
- De Wit, J., De Winter, F., Klooster, J., and Verhaagen, J. (2005). Semaphorin 3A displays a punctate distribution on the surface of neuronal cells and interacts with proteoglycans in the extracellular matrix. *Mol. Cell. Neurosci.* 29, 40–55.
- de Wit, J., Toonen, R.F., and Verhage, M. (2009). Matrix-dependent local retention of secretory vesicle cargo in cortical neurons. *J. Neurosci.* 29, 23–37.
- Demyanenko, G.P., Riday, T.T., Tran, T.S., Dalal, J., Darnell, E.P., Brennaman, L.H., Sakurai, T., Grumet, M., Philpot, B.D., and Maness, P.F. (2011). NrCAM deletion causes topographic mistargeting of thalamocortical axons to the visual cortex and disrupts visual acuity. *J. Neurosci.* 31, 1545–1558.
- Fournier, A.E., Nakamura, F., Kawamoto, S., Goshima, Y., Kalb, R.G., and Strittmatter, S.M. (2000). Semaphorin3A enhances endocytosis at sites of receptor-F-actin colocalization during growth cone collapse. *J. Cell Biol.* 149, 411–422.
- Freund, T.F., and Buzsáki, G. (1996). Interneurons of the hippocampus. *Hippocampus* 6, 347–470.
- Garver, T.D., Ren, Q., Tuvia, S., and Bennett, V. (1997). Tyrosine phosphorylation at a site highly conserved in the L1 family of cell adhesion molecules abolishes ankyrin binding and increases lateral mobility of neurofascin. *J. Cell Biol.* 137, 703–714.
- He, Z., and Tessier-Lavigne, M. (1997). Neuropilin is a receptor for the axonal chemorepellent Semaphorin III. *Cell* 90, 739–751.
- Hoshino, M., Nakamura, S., Mori, K., Kawauchi, T., Terao, M., Nishimura, Y.V., Fukuda, A., Fuse, T., Matsuo, N., Sone, M., et al. (2005). Ptf1a, a bHLH transcriptional gene, defines GABAergic neuronal fates in cerebellum. *Neuron* 47, 201–213.
- Huang, Z.J., Di Cristo, G., and Ango, F. (2007). Development of GABA innervation in the cerebral and cerebellar cortices. *Nat. Rev. Neurosci.* 8, 673–686.
- Janssen, B.J., Malinauskas, T., Weir, G.A., Cader, M.Z., Siebold, C., and Jones, E.Y. (2012). Neuropilins lock secreted semaphorins onto plexins in a ternary signaling complex. *Nat. Struct. Mol. Biol.* 19, 1293–1299.
- Kriebel, M., Metzger, J., Trinks, S., Chugh, D., Harvey, R.J., Harvey, K., and Volkmer, H. (2011). The cell adhesion molecule neurofascin stabilizes axo-axonic GABAergic terminals at the axon initial segment. *J. Biol. Chem.* 286, 24385–24393.
- Law, C.O., Kirby, R.J., Aghamohammadzadeh, S., and Furley, A.J. (2008). The neural adhesion molecule TAG-1 modulates responses of sensory axons to diffusible guidance signals. *Development* 135, 2361–2371.
- Lee, W.C., Huang, H., Feng, G., Sanes, J.R., Brown, E.N., So, P.T., and Nedivi, E. (2006). Dynamic remodeling of dendritic arbors in GABAergic interneurons of adult visual cortex. *PLoS Biol.* 4, e29.
- Lein, E.S., Hawrylycz, M.J., Ao, N., Ayres, M., Bensinger, A., Bernard, A., Boe, A.F., Boguski, M.S., Brockway, K.S., Byrnes, E.J., et al. (2007). Genome-wide atlas of gene expression in the adult mouse brain. *Nature* 445, 168–176.
- Li, W.C., Cooke, T., Sautois, B., Soffe, S.R., Borisjuk, R., and Roberts, A. (2007). Axon and dendrite geography predict the specificity of synaptic connections in a functioning spinal cord network. *Neural Dev.* 2, 17.
- Packer, A.M., and Yuste, R. (2011). Dense, unspecific connectivity of neocortical parvalbumin-positive interneurons: a canonical microcircuit for inhibition? *J. Neurosci.* 31, 13260–13271.
- Palay, S.L., and Chan-Palay, V. (1974). *Cerebellar Cortex: Cytology and Organization* (Springer-Verlag).
- Porter, J.T., Johnson, C.K., and Agmon, A. (2001). Diverse types of interneurons generate thalamus-evoked feedforward inhibition in the mouse barrel cortex. *J. Neurosci.* 21, 2699–2710.

- Ramon y Cajal, S. (1911). *Histologie du Systeme Nerveux de l'Homme et des Vertebres* (Maloine).
- Saywell, V., Cioni, J.M., and Ango, F. (2014). Developmental gene expression profile of axon guidance cues in Purkinje cells during cerebellar circuit formation. *Cerebellum* *13*, 307–317.
- Shimizu, M., Murakami, Y., Suto, F., and Fujisawa, H. (2000). Determination of cell adhesion sites of neuropilin-1. *J. Cell Biol.* *148*, 1283–1293.
- Sotelo, C. (2008). Viewing the cerebellum through the eyes of Ramón y Cajal. *Cerebellum* *7*, 517–522.
- Stepanyants, A., Tamás, G., and Chklovskii, D.B. (2004). Class-specific features of neuronal wiring. *Neuron* *43*, 251–259.
- Takagi, S., Kasuya, Y., Shimizu, M., Matsuura, T., Tsuboi, M., Kawakami, A., and Fujisawa, H. (1995). Expression of a cell adhesion molecule, neuropilin, in the developing chick nervous system. *Dev. Biol.* *170*, 207–222.
- Tamás, G., Lorincz, A., Simon, A., and Szabadics, J. (2003). Identified sources and targets of slow inhibition in the neocortex. *Science* *299*, 1902–1905.
- Taniguchi, M., Yuasa, S., Fujisawa, H., Naruse, I., Saga, S., Mishina, M., and Yagi, T. (1997). Disruption of semaphorin III/D gene causes severe abnormality in peripheral nerve projection. *Neuron* *19*, 519–530.
- Uesaka, N., Uchigashima, M., Mikuni, T., Nakazawa, T., Nakao, H., Hirai, H., Aiba, A., Watanabe, M., and Kano, M. (2014). Retrograde semaphorin signaling regulates synapse elimination in the developing mouse brain. *Science* *344*, 1020–1023.
- Volkmer, H., Zacharias, U., Nörenberg, U., and Rathjen, F.G. (1998). Dissection of complex molecular interactions of neurofascin with axonin-1, F11, and tenascin-R, which promote attachment and neurite formation of tectal cells. *J. Cell Biol.* *142*, 1083–1093.
- Wierenga, C.J., Becker, N., and Bonhoeffer, T. (2008). GABAergic synapses are formed without the involvement of dendritic protrusions. *Nat. Neurosci.* *11*, 1044–1052.
- Wong, C.W., Wiedle, G., Ballestrem, C., Wehrle-Haller, B., Etteldorf, S., Bruckner, M., Engelhardt, B., Gisler, R.H., and Imhof, B.A. (2000). PECAM-1/CD31 trans-homophilic binding at the intercellular junctions is independent of its cytoplasmic domain; evidence for heterophilic interaction with integrin α v β 3 in *Cis*. *Mol. Biol. Cell* *11*, 3109–3121.
- Wright, A.G., Demyanenko, G.P., Powell, A., Schachner, M., Enriquez-Barreto, L., Tran, T.S., Polleux, F., and Maness, P.F. (2007). Close homolog of L1 and neuropilin 1 mediate guidance of thalamocortical axons at the ventral telen-cephalon. *J. Neurosci.* *27*, 13667–13679.
- Yamagata, M., and Sanes, J.R. (2008). Dscam and Sidekick proteins direct lamina-specific synaptic connections in vertebrate retina. *Nature* *451*, 465–469.
- Yamano, M., and Tohyama, M. (1994). Distribution of corticotropin-releasing factor and calcitonin gene-related peptide in the developing mouse cerebellum. *Neurosci. Res.* *19*, 387–396.
- Zonta, B., Desmazieres, A., Rinaldi, A., Tait, S., Sherman, D.L., Nolan, M.F., and Brophy, P.J. (2011). A critical role for Neurofascin in regulating action potential initiation through maintenance of the axon initial segment. *Neuron* *69*, 945–956.

Neuron, Volume 91

Supplemental Information

**Dual Function of NRP1 in Axon Guidance
and Subcellular Target Recognition in Cerebellum**

Ludovic Telley, Christelle Cadilhac, Jean-Michel Cioni, Veronique Saywell, Céline Jahannault-Talignani, Rosa E. Huettl, Catherine Sarrailh-Faivre, Alexandre Dayer, Andrea B. Huber, and Fabrice Ango

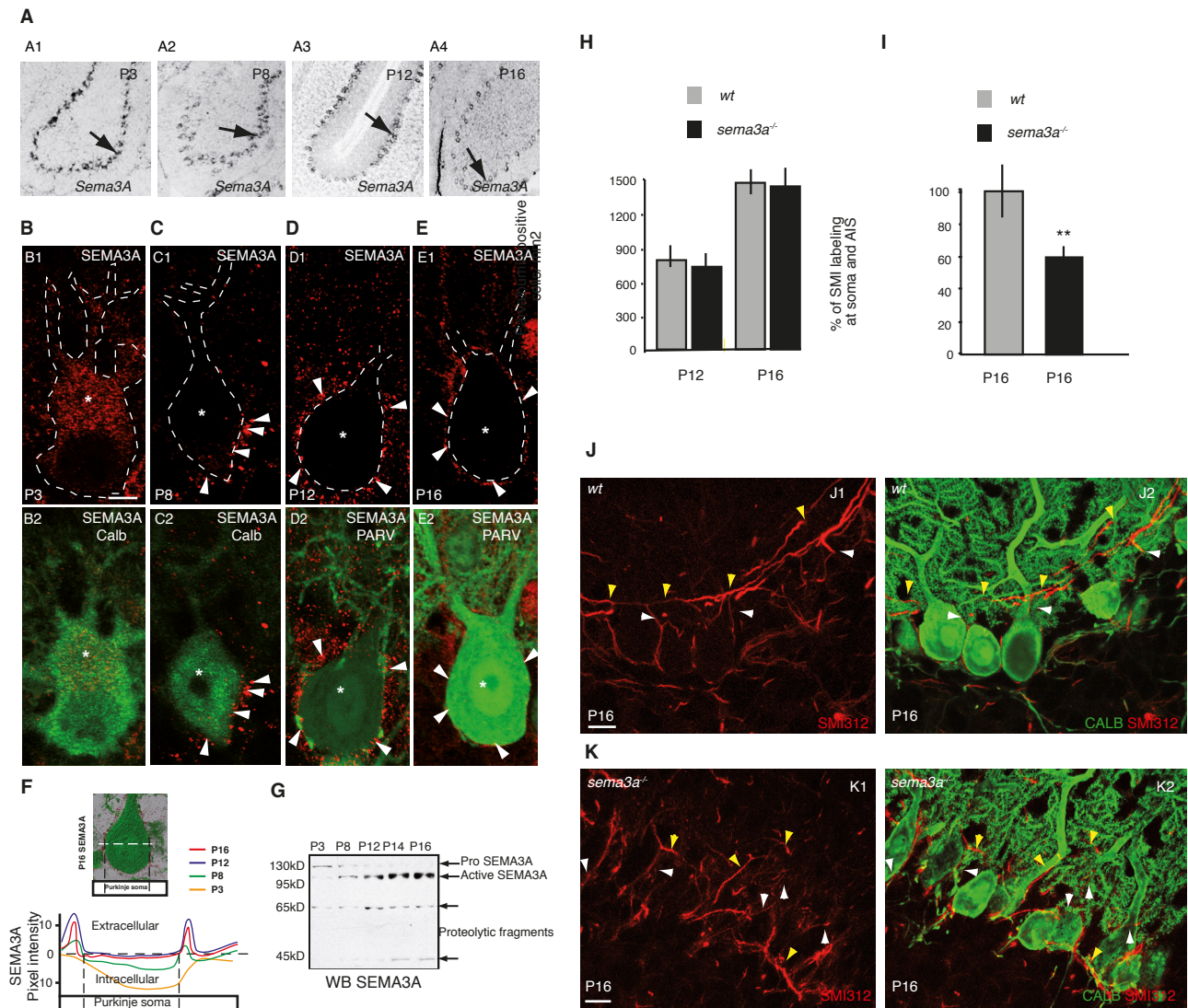


Figure S1, related to Figure 1. SEMA3A expression by Purkinje cells and GABAergic axon organization.

(A) In situ hybridization of *Sema3a* on cerebellar cortex at P3 (A1), P8 (A2), P12 (A3) and P16 (A4). Arrows point to PCL positive signals. Confocal images of endogenous SEMA3A (red) and PCs revealed with calbindin (Calb) or parvalbumin (Parv) antibodies (green) at P3 (B1-2), P8 (C1-2), P12 (D1-2) and P16 (E1-2). Note the expression of SEMA3A in PC soma (star) at P3 (B1). Arrowheads in C, D and E showed SEMA3A punctate accumulation around PC body. F1 is an example of a 3D rendering of PC (green) and SEMA3A (red) used for SEMA3A pixel intensity measurement along the dotted white line and quantified in F at P3, P8, P12 and P16. The horizontal dotted black line delineated intra and extracellular expression of SEMA3A. The vertical dotted lines delineated the PC soma. (G) Cerebellum at P3, P8, P12 and P16 were lysed and immunoblotted for SEMA3A protein expression. Four different forms of SEMA3A were dynamically observed during development, the ProSEMA3A isoform (125kD), the active isoform (92kD) and the proteolytic isoforms (65/45 kD). (H) Quantification of Parv positive cells in the ML at P12 and P16 of wt and *sema3a^{-/-}* mice. BCs axons labeled with SMI-312 (J, K) in wt (J) and *sema3a^{-/-}* deficient mice (K) at P16. PCs are labeled with calbindin (green, J2, K2). White arrowheads show BCs axons at soma. Yellow arrowheads show BCs axon main shafts. BCs axons at both soma and AIS were quantified by using SMI-312 labeling at P16 (I, **: n=14, P=0.0045, Student t-test). Scale bars represent 10 μ m.

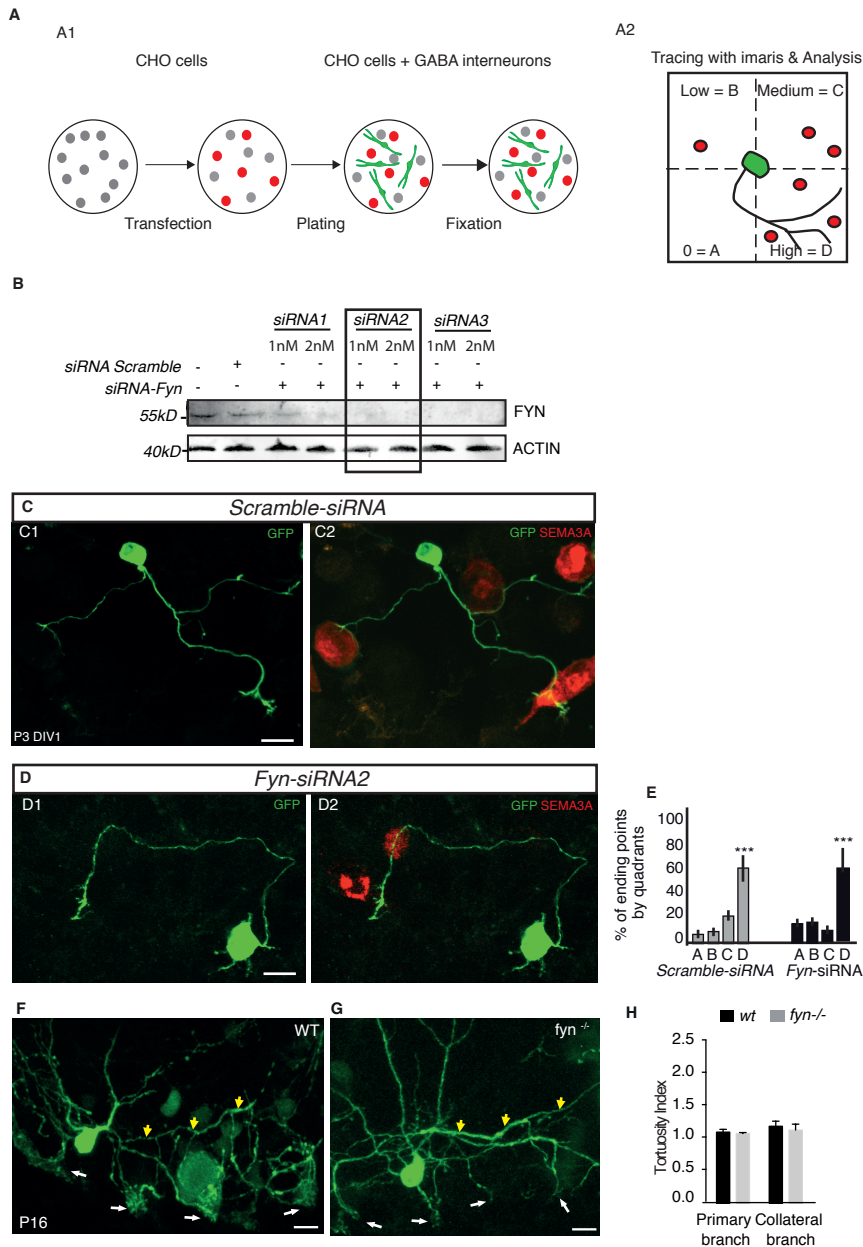
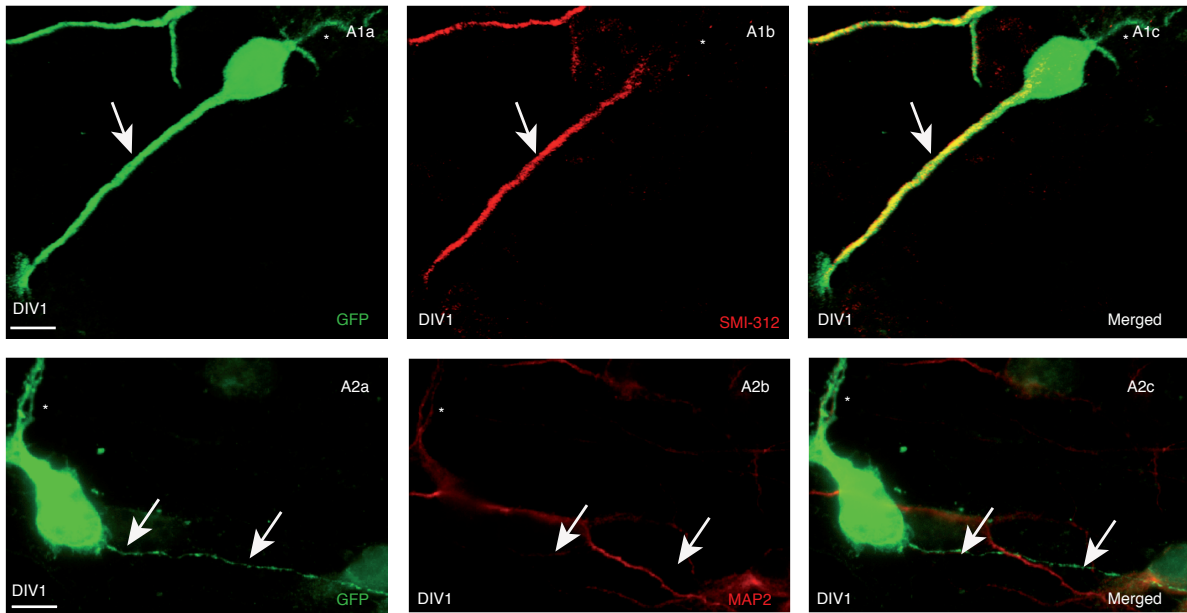


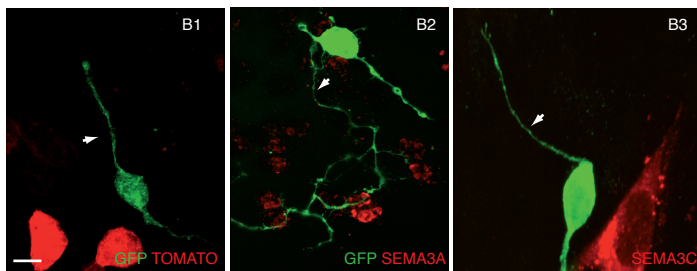
Figure S2, related to Figure 2. SEMA3A attracts BCs axon in SEMA3A/FYN deficient signaling cells.

(A) Schematic representation of the co-culture model. 24h after CHO cells transfection, GABAergic interneurons (green) from *gad67-gfp* mice were plated on the top of CHO cells. Red and grey dots are transfected and untransfected CHO cells respectively (A1). To quantify axons or axon branches preferential localization, images were separated in four equivalent quadrants centered on the neuron soma (A2). The number of branches was counted in each quadrant and scored against the pixel intensity of CHO cells. (B) Western-blot of FYN expression in the presence of *Scramble* and three different *Fyn* siRNA. (C) In this striking example of co-culture with SEMA3A, each BCs axon collateral follows a specific path towards cells expressing SEMA3A (red, C2). In *Fyn* deficient interneurons, SEMA3A failed to induce axon branches but the guidance is not affected. Note the change in axon directionality towards SEMA3A positive cells (D). (E) Quantification of BCs axon endings in both conditions revealed that quadrant with high SEMA3A expression level correlates with highest percentage of axonal endings (***: n= 20 cells per condition; P=0.0004 (*Scramble*-siRNA) and 0.0009 (*Fyn*-siRNA), Two-way Anova) In WT (F) or *fyn* KO mice (G), both primary and collateral branches displayed the same tortuosity index as quantified in H. Scale bars represent 10 μ m.

A



B



C

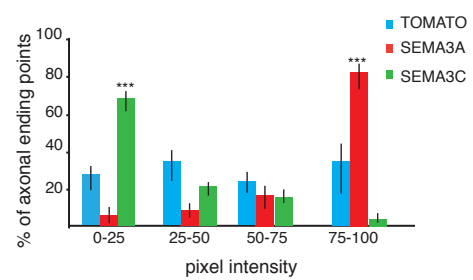


Figure S3, related to Figure 2. Specificity of SEMA3A effect in vitro. After one day in co-culture, GFP positive interneurons (green, A1a and A2a) are already differentiated with axons labeled with SMI-312 (red, A1b) and dendrites labeled with MAP2 (red, A2b). Merged images of A1 and A2 are presented in A1c and A2c respectively. White stars indicate dendritic domain and white arrows point to axons. CHO cells transfected with SEMA3A (red, B2) or SEMA3C (red, B3) attracted (C, ***, $n=18$; $P=0.0006$, Student t-test) or repelled (C, ***, $n=15$; $P=0.0009$, Student t-test) respectively GABAergic axons as compared to control CHO cells transfected with TOMATO (red, B1) and as quantified in (C). Scale bars represent 10 μm .

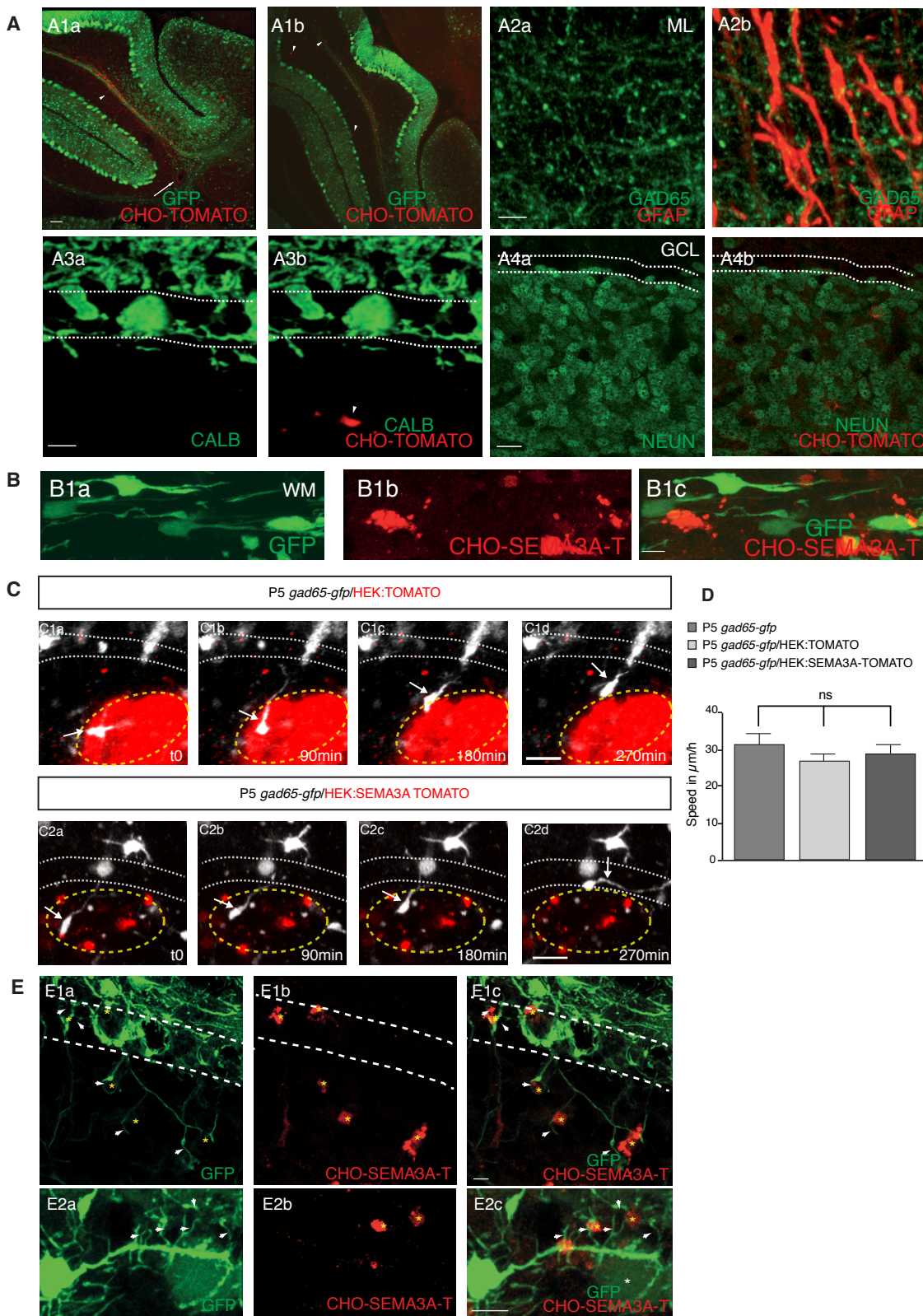


Figure S4, related to Figure 2

Normal cerebellar cytoarchitecture and GABAergic interneuron migration after heterologous cells injection *in vivo* but altered BCs axon organization in the presence of SEMA3A ectopic expression.

After 7 to 14 days post-injection, CHO cells are localized in different layers of the cerebellum (white arrowheads in A). The injection site is pointed with a white arrow (A1a). Cerebellum were cut into serial 100 μm -thick vibratome sagittal slices, (A1a-b). Note the diffusion of CHO cells away from the injection site in the same cerebellar folium. Injection of CHO cells that expressed TOMATO in cerebellar cortex did not alter major cellular organization in the ML (A1, A2), PCL (A1, A3), GCL (A1, A4) and WM (A1, A5). GAD65 punctates (green, A2) appeared normal and colocalized with GFAP in ML as previously described (Ango et al. 2008). Normal localization of granule cells labeled with NeuN is observed in the GCL (green, A4). Localization of CHO cells in the WM does not perturb interneurons migration that displayed normal morphology in fixed cerebellum (green, B1a-c). Time-lapse imaging performed in *gad65-gfp* mice injected with HEK cells expressing TOMATO (C1a-d) or SEMA3A-TOMATO (C2a-d) showed the same migration behavior with comparable migration speed (D). CHO grafts in ML (E1 and E2), PCL (E1 and E2) or GCL (E1) induced BCs axon reorganization. (E1-E2) White arrows point to BCs collaterals that grew either downward (E1a-c) or upward towards ML SEMA3A-expressing CHO cells (E2; yellow stars). Note that BCs axons grew towards SEMA3A-expressing CHO cells (yellow stars) localized in PCL or GCL (E1, E2). Dashed lines delineated the PCL. Scale bars represent 10 μm .

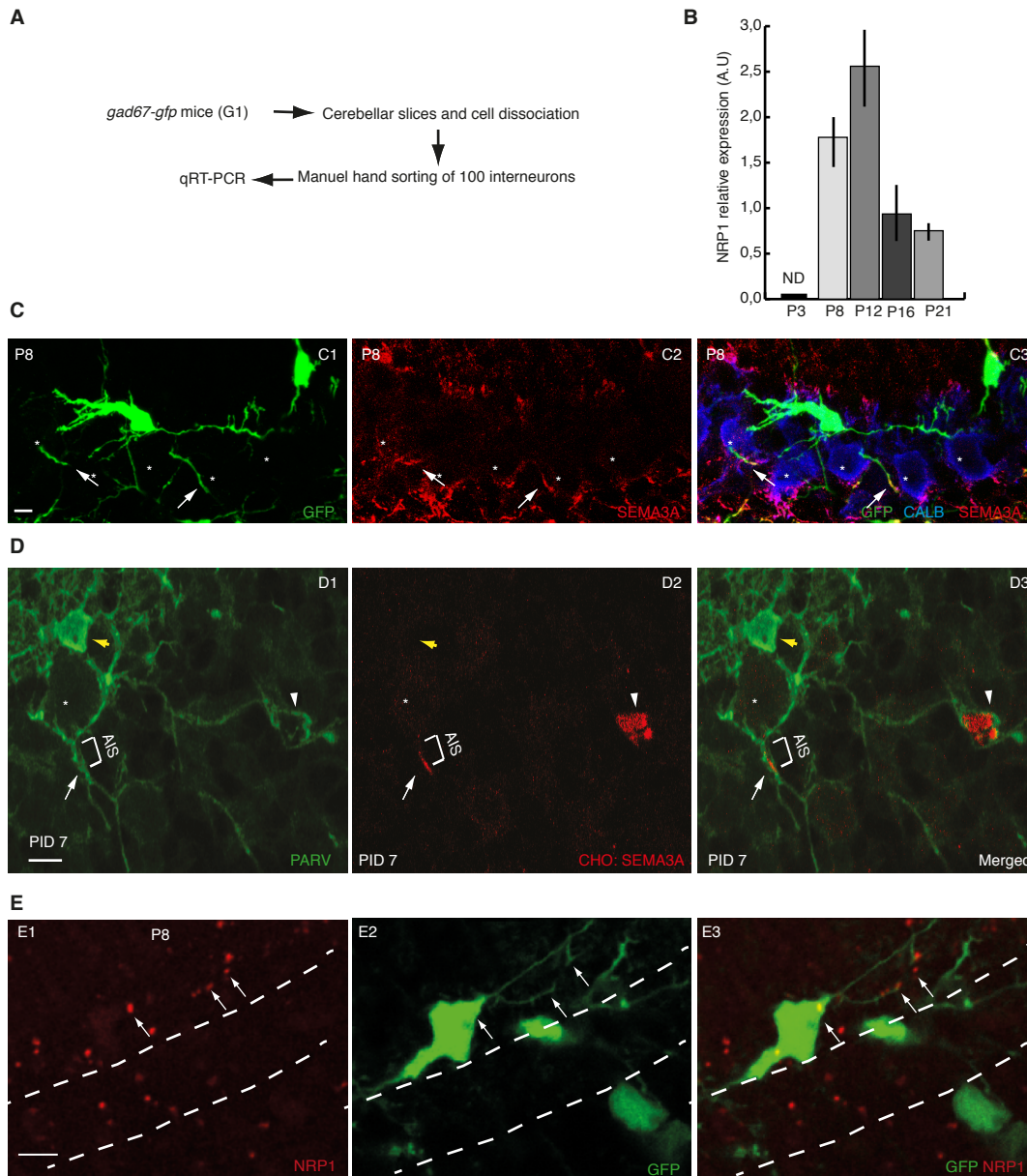


Figure S5, related to Figure 3. SEMA3A receptor is expressed by BCs and preferentially localized in pinceau synapse. (A) Rapid description of the experiment to analyze the expression of *Nrp1* mRNA in BCs using qRT-PCR. (B) *Nrp1* mRNA relative expression at P3, P8, P12, P16 and P21. (C) P8 *gad67:gfp* (C1) immunohistochemistry of SEMA3A (C2) shows local stabilization of SEMA3A around PCs labeled with CALB (C3, *). Arrows show SEMA3A accumulation on BCs axon endings. (D) In vivo localization of SEMA3A-TOMATO secreted by grafted CHO cells accumulated at pinceau, assuming the presence of a receptor for SEMA3A. White stars: PC soma, white arrowheads: CHO cells, white arrows: SEMA3A-TOMATO accumulation at AIS, yellow arrow: BC soma. (E) PLA immunohistochemistry of NRP1 at P8 in young BCs. White arrows point to NRP1 expressed in both BCs soma and axons. Scale bars represent 10 μ m.

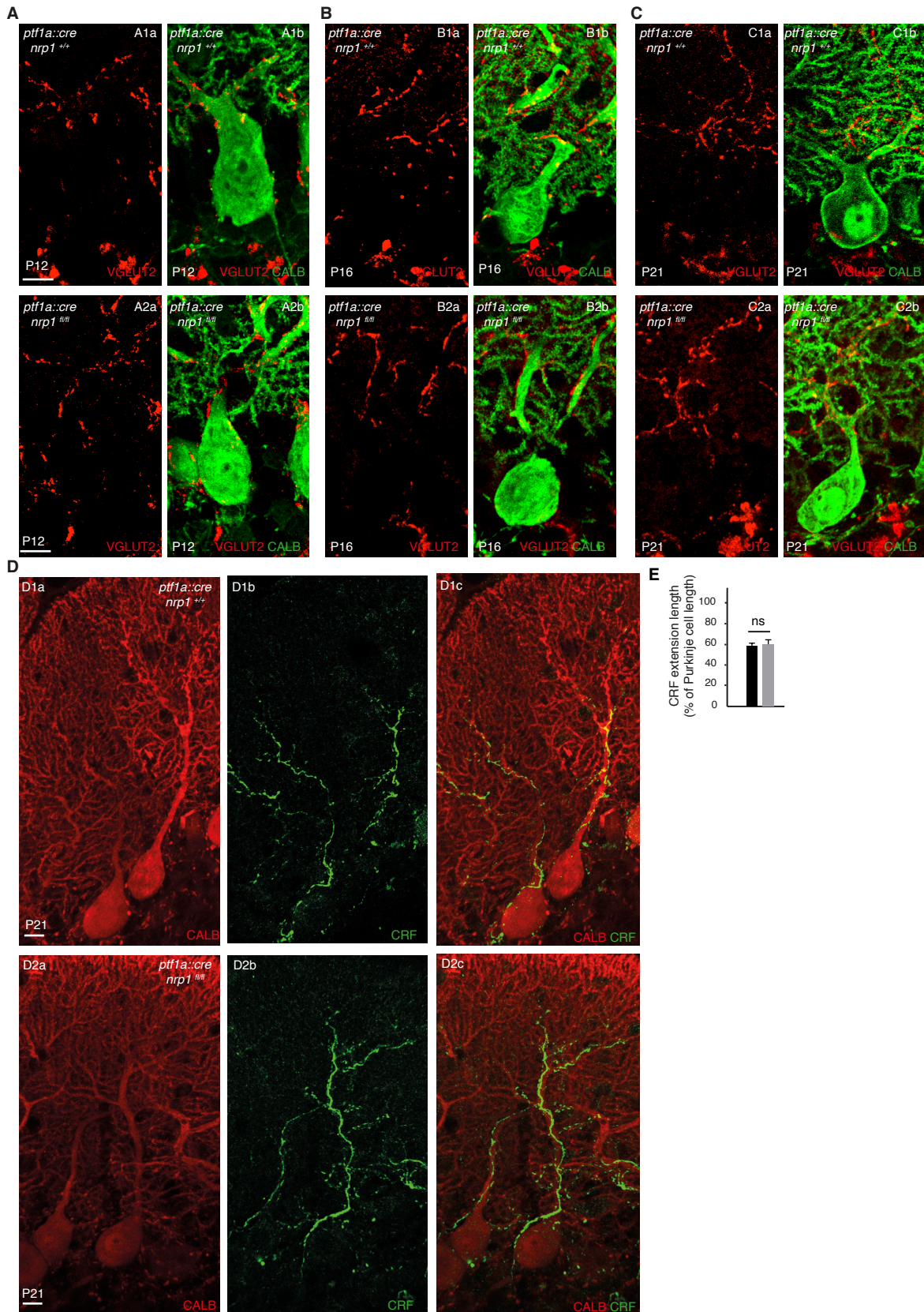


Figure S6, related to Figure 4. Climbing fiber synapses on PCs are not affected on *ptf1a::cre ; nrp1^{-/-}* mice. (A-C) Climbing fiber terminals are labeled with VGLUT2 (red, A-C), PCs labeled with CALB (green, A-C) at P12 (A) P16 (B) and P21 (C) in *ptf1a::cre ; nrp1^{fl/fl}* (A1, B1, C1) and *ptf1a::cre ; nrp1^{+/+}* (A2, B2, C2). (D) Climbing fibers labeled with corticotropin-releasing factor (CRF, green) show similar extension in the ML in both wt (D1) and *ptf1a::cre ; nrp1^{fl/fl}* (D2) mice and as quantified in E. Scale bars represent 10 μ m.

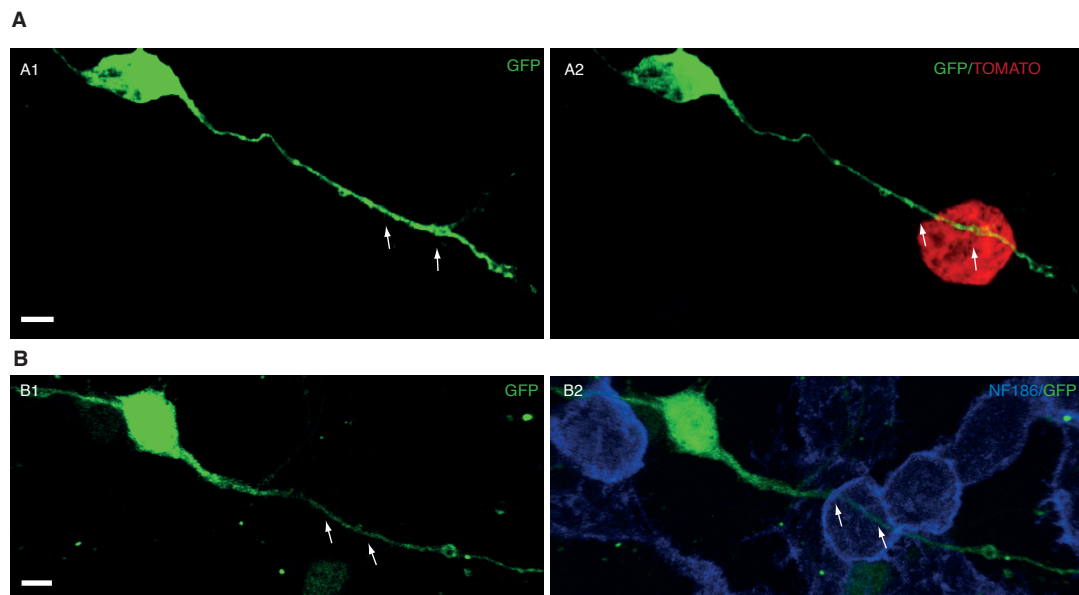


Figure S7, related to Figure 7. NF186 alone is not sufficient to induce target innervation. (A-C) Co-culture of GFP expressing interneurons mixed with CHO cells transfected with control TOMATO (red, A2) or NF186 (blue, B2). Note that interneuron axons (white arrows) show similar interaction with CHO cells expressing NF186 or TOMATO. Scale bars represent 10 μ m.

Supplemental method:

Animals and surgical procedures

The experimental plan was designed according to the European Communities Council Directive and the French law for care and use of experimental animals with authorization number: B 34-309 and approved protocol number: CEEA-LR-11031. For mixed coculture assay we used *gad67-gfp* BAC transgenic mice as previously described (Ango et al., 2004). For injection procedure, we used Swiss Webster (CFW®) mice. *Sema3a*^{-/-} mice were obtained from Riken Bioresource Center previously generated by (Taniguchi et al, 1997) MGI: 2158944. For *ptfla:cre;nrp1^{fl/fl}*, animals were handled and housed according to the federal guidelines for the use and care of laboratory animals, approved by the Helmholtz Zentrum München Institutional Animal Care and Use Committee and the Regierung von Oberbayern. The *nrp1^{fl/fl}* line is from (Gu et al., 2003), MGI identification number is MGI:3512101. The *ptfla:cre* mice are from (Nakhai et al., 2007), MGI identification number is MGI:3701996. The day of birth in this study is designated as postnatal day (P). All surgical procedures were performed under deep general anesthesia obtained by intraperitoneal administration of Ketamine (0,56mg/g of body weight) supplemented by Xylazine (0,03mg/g of body weight).

Plasmids.

Tomato-SEMA3A was generated by replacing EGFP in EGFP-SEMA3A (gift from Joost Verhaagen) by a fragment of 5'NHE1-TdTomato-BAMH13' amplified with primer :
AAAAAAAAAGCTAGCGCCACCATGGTGAGCAAG and
AAAAAAAAAGGATCCCTTGTACAGCTCGTCCATG on the sequence of PcmvTdTomato (Addgene).

In Situ Hybridization

The pBluescriptII-KS-semaIII (clone#52 – gift from Alain Chédotal) was linearized with Not1 (NEB-Biolabs) and used as a template for Digoxigenin-labelled antisens riboprobe synthesis with SP6 RNA polymerase (Promega) according to the supplier's instructions (Roche). Mouse brains were fixed as for immunohistochemistry and cryoprotected in saccharose 30% prior to cryosectioning. Free-floating cryostat sagittal sections (30µm thick) were processed for hybridization in 50% formamide, overnight at 65°C. Hybridization was detected using an alkaline phosphatase-coupled anti-Digoxigenin antibody (Roche 1:2000). Alkaline phosphatase staining was developed with NBT/BCIP (Roche) as a substrate.

Attraction analysis

Isolated interneurons with at least two transfected CHO cells in immediate proximity (≤ 150 μm) were chosen for analysis. Images of isolated interneurons were divided into four quadrants centered on the interneuron soma. For all quadrants, the relative fluorescence intensity of the transfected CHO was measured with ImageJ and normalized to the highest pixel value being 100%. The pixel intensity values were classified into 4 groups A (0-25%), B (25%-50%), C (50%-75%) and D (75-100%). The same analysis was done with interneurons whose number of ending points in each quadrant was quantified after 3D reconstruction using NeuroLucida software. The number of ending points was then scored against the pixel value intensity of the transfected protein. If our molecule of interest has an attractive function, a significant increase in the number of ending points is expected towards the quadrant with highest pixel intensity value (D), as compared to quadrants A, B and C. By contrast, if our molecule has a repulsive effect, the number of ending points should increase in quadrant (A) with the lowest protein expression.

Western blotting and Co-immunoprecipitation

HEK293 cells or mouse cerebellar tissues were lysed with solubilization buffer (HEPES 20 mM, NaCl 150 mM, 1% NP40, 10% glycerol, 4 mg/ml dodecylmaltoside, protease and phosphatase inhibitors) during 1h at 4°C under agitation. Then, samples were centrifuged and the supernatants were collected. For co-immunoprecipitation, lysates (HEK293 :0,5 mg ; Brain :1 mg) were incubated with NF186 specific antibody (rabbit polyclonal antibody, 2 $\mu\text{g/ml}$, Santa Cruz Biotech) for overnight at 4°C, and protein A Sepharose (GE Healthcare) or protein AG (protein Bio-Adembeads PAG, Ademtech) was added for 1h at 4°C. Proteins extracts were separated with 8% SDS-PAGE and transferred to nitrocellulose membranes (Hybond-C, Amersham Biosciences). Proteins were detected with primary antibodies overnight at 4°C, then washed and incubated with secondary antibodies for 1h at room temperature. The following antibodies were used: anti-pan-Actin (mouse monoclonal antibody, 1:2000, Cayman), anti-NF186 (rabbit polyclonal antibody, 1:1000, Abcam), anti-phosphotyrosine 4G10 (mouse monoclonal antibody, 1:500, Millipore), anti-Neuropilin1 (goat polyclonal antibody, 1:2000, R&D Systems). Immunoreactivity was detected using ECL Plus Western blotting Detection System, Amersham.

Time-lapse imaging.

P5 *gad65-gfp* mice brains were removed in ACSF (119 mM CaCl₂, 2,5 mM KCl, 2 mM MgCl₂, 2,5 mM CaCl₂, 1 mM Na₂HPO₄, 26,2 mM NaHCO₃, 20 mM glucose) and then cut in 300µm-thick slices with vibratome in frozen and oxygenated ACSF. After transfection of HEK cells with TOMATO or SEMA3A-TOMATO, inverted drops were prepared in order to form a cell layer. These drops were then cut into small pieces and inserted into the granule cell layer in the prepared slices, using a tungsten filament. The slices were then cultured with fresh Neurobasal medium supplemented with Glutamax (GIBCO), B27 (GIBCO) and a mix Penicillin/Streptomycin for recovery during 6 hours in the incubator. Finally, slices were imaged overnight with a confocal microscope (Nikon A1R, 20x, 37°C and 5% CO₂). Analyzes were done using the ImageJ MTrackJ plugin.

Microscopy and image processing.

All pictures were taken with a Zeiss confocal LSM780. Imaris software was used to adjust image contrast and assemble the final plates. Most quantitative and morphometric analysis were made using ImageJ (Research Service Branch, National Institutes of Health, Bethesda, MD; <http://rsb.info.nih.gov/ij/>) or Neurolucida (MWF Biosciences) which is used particularly to quantify and trace axons. For GAD65, Parv and SMI-312 local expression quantification, we measured the mean pixel intensity value in the PC layer using ImageJ and as previously described (Ango et al; 2004).

Axons were traced using Neurolucida software (Microbrightfield, Williston, Vermont, United States). From these tracings, we could easily derive data regarding axon tortuosity. The tortuosity index is the ratio of the true contour length of the axon segment (actual length) divided by the end-to-end distance (straight length) (Portera-Cailliau et al., 2005). The primary axon was identified as the main axonal branch attached to the soma. The secondary branches corresponded to axon collaterals issued by the primary axon.

List of antibodies used: Parvalbumin (1:1000; Chemicon), Calbindin (1:1000; Swant), GAD65 (1:300; Chemicon), GFAP (1:500; Dako), NeuN (1:200; Chemicon), VSV (1:500; Sigma), HA (1:300; Aves Lab), NF186 (1:1000 ; gift from Van Bennett), SEMA3A (1:100; Santa Cruz and 1:100; ECM Biosciences), MAP 2 (1:1000; Abcam), SMI-312 (1:200; Abcam), GFP (1:1500; Aves Labs), KV1.1 (1:100; Neuromab), HCN1 (1:100; Neuromab), NRP1 (1:300; R&D systems), VGLUT2 (1/2000; Millipore). Sections were incubated with either Alexa546-conjugated goat anti-mouse or anti-rabbit IgG and Alexa488-conjugated goat anti-rabbit, anti-chicken or anti-mouse IgG (1:500; Molecular Probes) 633-conjugated goat

anti-chicken (1:500; Millipore) and 546-conjugated rabbit anti-goat IgG (1:500; Molecular probes) and mounted.